Published in final edited form as:
*Nat Plants*. 2019 December ; 5(12): 1283–1296. doi:10.1038/s41477-019-0553-2.

# A novel eIF4E interacting protein that forms non-canonical translation initiation complexes

**René Toribio**[#1], **Alfonso Muñoz**[#1,3], **Ana B. Castro-Sanz**[#1], **Catharina Merchante**[2], **M. Mar Castellano**[*,1]

[1]Centro de Biotecnología y Genómica de Plantas. Universidad Politécnica de Madrid (UPM) - Instituto Nacional de Investigación y Tecnología Agraria y Alimentaria (INIA). Campus Montegancedo UPM. 28223-Pozuelo de Alarcón (Madrid), Spain

[2]Instituto de Hortofruticultura Subtropical y Mediterránea "La Mayora" - Universidad de Málaga-Consejo Superior de Investigaciones Científicas (IHSM-UMA-CSIC), Departamento de Biología Molecular y Bioquímica; Campus de Teatinos, 29071-Málaga, Spain

[#] These authors contributed equally to this work.

## Abstract

Translation is a fundamental step in gene expression that regulates multiple developmental and stress responses. One key step of translation initiation is the association between eIF4E and eIF4G. This process is regulated in different eukaryotes by proteins that bind to eIF4E; however, evidence of eIF4E interacting proteins able to regulate translation is missing in plants. Here, we report the discovery of CERES, a plant eIF4E interacting protein. CERES contains an LRR domain and a canonical eIF4E binding site (4E-BS). Although the CERES/eIF4E complex does not include eIF4G, CERES forms part of cap-binding complexes, interacts with eIF4A, PABP and eIF3 and co-sediments with translation initiation complexes *in vivo*. Moreover, CERES promotes translation *in vitro* and general translation *in vivo,* while it modulates the translation of specific mRNAs related to light- and carbohydrate-response. These data suggest that CERES is a non-canonical translation initiation factor that modulates translation in plants.



[*]Corresponding author: Castellano M.M. castellano.mar@inia.es.
[3]Present address: Departamento de Botánica, Ecología y Fisiología Vegetal. Campus de Rabanales. Edificio Severo Ochoa, Universidad de Córdoba, 14071-Córdoba, Spain

**Reporting Summary**
Further information on research design is available in the Nature Research Reporting Summary linked to this article.

**Data availability**
The data that support the findings of this study are available from the corresponding author upon reasonable request. In addition, Super-resolution profile data are deposited in Gene Expression Omnibus database (GEO-NCBI) (http://www.ncbi.nlm.nih.gov/geo/) with accession code: GSE124290 (https://www.ncbi.nlm.nih.gov/geo/query/acc.cgi?acc=GSE124290).

**Author Contribution**
R.T., A.M. and M.M.C. designed most of the experiments. A.B.C-S. also contributed to the experimental design. R.T., A.M., A.B.C-S. and M.M.C performed the experiments and analysed the data; C.M. helped to perform a preliminary super-resolution ribosome profiling analysis. M.M.C wrote the manuscript with the help of A.M and R.T. All of the authors revised and approved the manuscript.

**Competing Interest**
Authors declare no conflict of interest.


Europe PMC Funders Author Manuscripts

Most eukaryotic mRNAs are translated by a cap-dependent mechanism, whereby the 5′-cap structure ($m^7$GpppN, where N is any nucleotide) is recognised by the eukaryotic translation initiation factor 4E (eIF4E). eIF4E forms a complex with eIF4G, a scaffolding protein that interacts with the DEAD-box RNA helicase eIF4A. The association of eIF4E, eIF4G and eIF4A generates the so-called eIF4F complex. In addition, eIF4G also binds to, among other factors, the poly(A)-binding protein (PABP) and eIF3, which allow mRNA recircularisation and the loading of the 43S preinitiation complex, leading to translation initiation [1–3].

Due to its crucial role in recruiting mRNAs to the ribosome, the eIF4E/eIF4G interaction is a central target of translational control in different eukaryotes. eIF4G interacts with the dorsal surface of eIF4E through the so-called eIF4E-binding site (4E-BS). This motif is characterised by a minimal canonical sequence YXXXXLϕ (where X is any residue and ϕ is any hydrophobic amino acid). This sequence, which has been recently extended to YX(R/K)XXLϕ(R/K/Q) [4], is also found in different eIF4E interacting proteins [5], such as the 4E-binding proteins (4E-BPs), EAP1, p20, Cup and Neuroguidin, which generally function as translational repressors by acting as competitive inhibitors of eIF4G binding [6–12].

Plants are characterised by the presence of two distinct isoforms of eIF4E (named eIF4E and eIF(iso)4E). These eIF4E isoforms selectively engage with eIF4G and eIF(iso)4G in the eIF4F and eIF(iso)4F complexes, respectively [13,14]. Along with these complexes, eIF4A has been shown to be part of the cap-binding complex in Arabidopsis proliferating cells [15].

In plants, translation is highly regulated during different developmental programs and in response to multiple stimuli [16–18]. Among these stimuli, different studies have reported that translation cycles in response to light [19–21]. Despite the well-known relevance of regulation of translation in plants, the mechanisms involved in translational control in these eukaryotes remain mainly unknown. In this sense, different studies have pointed out that some of the main mechanisms for translation regulation in mammals and fungi are missing in plants and some others that seem to be conserved show a different level of specialisation [22,23]. Interestingly, one of the mechanisms whose existence has been continuously questioned in the plant kingdom is the one that regulates in other eukaryotes the formation of the eIF4E/eIF4G complexes through the competitive binding to eIF4E[14,24]. Indeed, no clear homologues of the yeast and metazoan eIF4E translational regulators have been found in plant genomes to date [6–12,25]. More importantly, it has been described that in plants the interaction between the components of the eIF4F and eIF(iso)4F complexes is at the nanomolar to subnanomolar level, which makes unlikely that these complexes readily dissociate once formed [13]. In addition, although different proteins that contain a canonical 4E-BS and bind eIF4E and eIF(iso)4E have been described in Arabidopsis and wheat (such as LOX2, BTF3, CBE1 or EXA1) [26–30], their direct role in translation has not been proven, leaving the existence of possible analogues or completely new eIF4E translational regulators unexplored.

In this study, we describe the existence of a novel eIF4E interacting protein (called CERES). Our results indicate that CERES acts as a non-canonical translation initiation factor that interacts with eIF4E isoforms (through a conserved 4E-BS) and, in the absence of eIF4G isoforms, recruits eIF4A, eIF3 and PABP. The effect of CERES in translation is observed at

specific stages of the diurnal cycle, such as zeitgeber time 5, ZT5, a condition where the metabolic and nutritional status of the plant is at its highest level or close to it. At this time point, polysomal profiles and super-resolution ribosome profiling suggest that CERES boosts general translation and fine-tunes the specific translation of a set of mRNAs involved in light response and saccharide management. Consistent with this observation, *ceres* mutants show a hypersensitive phenotype in response to high glucose concentrations. These data suggest that, in contrast to other eIF4E interacting proteins, which mainly inhibit translation in other eukaryotes, CERES boosts general translation at ZT5, when metabolic and translational conditions are favourable in the cell.

## Results

### CERES is an uncharacterised eIF4E interacting protein in plants

In order to identify proteins that could interact with AteIF4E and could modulate its function in translation in plants, we performed a yeast two-hybrid screening of an Arabidopsis Gal4 expression library using the full-length AteIF4E1 as bait. This analysis yielded 45 positive clones able to grow in highly stringent selective medium. Among them, we retrieved a partial cDNA clone of AteIF4G encompassing the eIF4G´s 4E-BS, which indicated that our screening was valid to identify eIF4E interacting proteins. In addition to eIF4G, a high percentage of these positive clones (20 out of 45) corresponded to partial cDNA clones of an Arabidopsis protein (At4g23840) predicted to belong to the Leucine-rich repeat (LRR) family. This uncharacterised protein was named CERES after the Roman goddess of agriculture. As shown in Fig. 1a, the growth of the original clones expressing eIF4E1 and the truncated versions of CERES or eIF4G was maintained at high concentrations of 3-amino-1,2,4-triazole (3-AT). In addition, the interaction between full-length CERES and eIF4E1 and eIF(iso)4E was confirmed using CERES as bait by directed two-hybrid assays (Fig. 1b and Extended Data Fig. 1a), demonstrating that CERES interacts with eIF4E1 and AteIF(iso)4E in the yeast two-hybrid system.

### CERES localises at the same subcellular locations as the eIF4E proteins and interacts with eIF4E1 and eIF(iso)4E *in planta*

In order to further characterise CERES interaction with eIF4E1 and eIF(iso)4E *in planta*, we firstly evaluated if CERES shares the same subcellular localisation as these translation initiation factors. To do so, the construct *pCERES:CERES-GFP* was transiently expressed in *N. benthamiana* leaves, where the correct size and integrity of the fusion protein was tested (Extended Data Fig. 2a). As shown in Fig. 1c upper panel, and consistent with the predicted localisation in the SUBA database, CERES is localised in the cytoplasm and the nucleus. To further corroborate that this localisation is the same as the one displayed by the eIF4E translation initiation factors, we repeated the same experiment co-expressing the constructs *pCERES:CERES-GFP* along with *p35S:RFP-eIF4E1*. As shown in Fig. 1c bottom panels, both proteins are specifically localised in the cytoplasm and nucleus, sharing the same subcellular localisation. These results along with the yeast two-hybrid data reinforced our hypothesis that CERES could interact with eIF4Es *in planta*.

To definitively verify their possible interaction *in vivo,* we agroinfiltrated *N. benthamiana* leaves with different combinations of the constructs *p35S:HA-CERES, p35S:Flag-eIF4E1* and *p35S:Flag-eIF(iso)4E* and we carried out eIF4E1 or eIF(iso)4E immunoprecipitations using anti-Flag beads. As shown in Fig. 1d, CERES is only co-immunoprecipitated in the presence of eIF4E1 and eIF(iso)4E. Similar results were obtained when the epitopes fused to the proteins were swapped and CERES was immunoprecipitated (Extended Data Fig. 1b). These data demonstrate that CERES interacts with eIF4E1 and eIF(iso)4E *in planta*.

## CERES seems to be a plant-specific protein and contains a highly conserved 4E-BS

*CERES* encodes a 597 aa protein with a predicted molecular mass of 65.76 kDa and contains 15 LRR repetitions that stretch from the amino acid 88 to 510 (Fig. 2a). Interestingly, CERES also shows an YNREELVALQ motif (amino acids 563-572) that matches the extended consensus sequence of the canonical eIF4E binding site [YX(R/K)XXLϕXX(R/K/Q)] (Fig. 2b). This domain was present in all the truncated original clones obtained in the yeast two-hybrid screening. No other paralogues have been found in the Arabidopsis databases, revealing that *CERES* is a single-copy gene in this plant species. qRT-PCR analysis of *CERES* mRNA expression showed that this novel gene is expressed in whole seedlings and seedlings´ roots, leaves, stem and flowers from adult plants (Extended Data Fig. 3).

No CERES orthologues (in terms of proteins sharing high homology with the CERES´ LRR domains that also contain a canonical 4E-BS) were identified by BLAST analysis in other eukaryotes outside the plant kingdom. In contrast, this analysis retrieved CERES homologues in all analysed plant genomes from bryophytes to angiosperms. These proteins share >35% identity and >95% coverage with AtCERES, with the exception of *Picea sitchensis* CERES, which has a lower coverage (73%), since it lacks the first 152 amino acids of the Arabidopsis sequence.

Remarkably, the canonical 4E-BS present in AtCERES is highly conserved among all CERES orthologues in plants (Fig. 2b). Indeed, alignment profiles show that the invariant Y and the hydrophobic residue at position +7 of the minimal 4E-BS canonical site (YXXXXLØ) are fully conserved, while the Leu at position +6 is either conserved or replaced by another hydrophobic amino acid. These proteins also display a high conservation of the Arg/Lys residues at positions +3 and Arg/Lys/Gln residues at position +10 included in the extended consensus 4E-BS sequence [4]. The conservation of this binding site among plant species strongly suggests that the 4E-BS could be especially relevant for CERES function.

## The 4E-BS is essential for CERES interaction with AteIF4E isoforms

In other organisms, the interaction between eIF4E and different 4E interacting proteins is mediated by the 4E-BS [5,22]. Therefore, we analysed if the canonical 4E-BS present in CERES was critical for the interaction between CERES and the AteIF4E isoforms. To do so, we generated a CERES version that contains a deletion of the core of the canonical 4E-BS (CERESΔ563-570) (Fig. 2c, upper scheme) and assayed the capacity of this mutant to interact with AteIF4E1 and AteIF(iso)4E in the yeast two-hybrid system. Although

CERESΔ563-570 is expressed in yeast to similar levels as its wild-type counterpart (Extended Data Fig. 2b), the deletion of CERES´ 4E-BS completely abolished eIF4E1 or eIF(iso)4E binding (Fig. 2d). In order to corroborate the requirement of a functional 4E-BS for CERES interaction with eIF4E *in vivo*, we generated the constructs *p35S:HA-CERES*$^{Y563A}$ and *p35S:HA-CERESΔ563-570* to allow the expression *in planta* of two mutant versions of CERES, one containing a single substitution of Tyr563 to Ala (Y563A) and the other lacking the minimal 4E-BS, respectively (Fig. 2c). These constructs were co-expressed along with *p35S:Flag-eIF4E1* in *N. benthamiana* leaves and protein interaction was analysed by co-immunoprecipitation. As shown in Fig. 2e, compared to the wild-type CERES, the interaction with AteIF4E1 was drastically reduced when CERES$^{Y563A}$ was assayed. Furthermore, this interaction was fully abolished in the case of the CERESΔ563-570. Similar results were obtained for AteIF(iso)4E; however, in this case the single Y563A substitution was enough to preclude the eIF(iso)4E binding, suggesting that the interaction with CERES is weaker for eIF(iso)4E (Fig. 2f).

All these data demonstrate that the 4E-BS of CERES is required for its interaction with AteIF4E1 and AteIF(iso)4E *in vivo*.

## CERES, through its interaction with eIF4E, forms part of a complex that binds the cap structure

eIF4E factors are involved in the recognition of the RNA cap structure. So, to further explore the possible role of CERES as an eIF4E interacting protein, we analysed the capacity of CERES to be part of cap-binding complexes. To do so, we expressed AteIF4E1, AteIF(iso)4E and CERES proteins fused to the GST tag in *E. coli*. From these assays, we were able to obtain an extremely low amount of soluble recombinant CERES that, although prevented its use in further experiments, was used to carry out affinity purifications from different mixtures of *E. coli* extracts with 7-methyl-GTP Sepharose. As shown in Extended Data Fig. 4, CERES was specifically retained in these columns in the presence of AteIF4E1 and AteIF(iso)4E, but not in the absence of the eIF4E isoforms, indicating that these factors may mediate the presence of CERES in cap-binding complexes.

In order to validate this observation by an independent approach, we expressed full-length CERES or a version of CERES that carries a deletion of the 4E-BS (CERESΔ563-570) in wheat germ extract (WGE) and the capacity of these proteins to be retained in a 7-methyl-GTP column was evaluated. It has to be noted that the WGE is a cell-free translation assay and, so, it is enriched in translation factors including the wheat (*Triticum aestivum*) TaeIF4E isoforms. As shown in Fig. 3a, only the full-length version of CERES is specifically retained in the 7-methyl-GTP column; however, this binding was drastically reduced when the version that lacks the 4E-BS (and which is unable to bind eIF4E isoforms) was assayed, reinforcing that CERES through its interaction with eIF4E binds to the cap structure.

Finally, the presence of CERES in cap-binding complexes was also analysed in Arabidopsis extracts. For this, polyclonal antibodies raised against the C-terminal part of AtCERES protein were generated and their capacity to recognise AtCERES was tested in extracts from Col-0 and from two independent T-DNA insertion lines in *CERES* gene (*ceres-1* and *ceres-2*). These lines displayed single insertions located in the third exon (*ceres-1*) and

second intron (*ceres-2*) of *CERES* (Extended Data Fig. 5a-b) and showed reduced levels of *CERES* mRNA compared to the wild-type plants by qRT-PCR (Extended Data Fig. 5c). Consistent with this result, western-blot analysis using the anti-AtCERES antibody showed that this antibody was able to recognise a band of ~ 66 kDa in Col-0 but not in the *ceres* mutants, indicating that the antibody is able to recognise the endogenous AtCERES protein and that these mutants are null or highly hypomorphic (Extended Data Fig. 5d). Using this antibody, the capacity of CERES to be retained with AteIF4E1 and AteIF(iso)4E in the 7-methyl-GTP resin or in the Sepharose resin (as control) was evaluated (Fig. 3b). As shown in this figure, the band corresponding to the endogenous AtCERES (which is absent in both *ceres* mutants) is specifically retained along with the eIF4E isoforms in the 7-methyl-GTP resin. However, none of these proteins are associated to the Sepharose resin, showing that these proteins are not retained in the matrix in the absence of the cap structure.

All together these data indicate that, through its interaction with eIF4E and eIF(iso)4E, CERES forms part of cap-binding complexes in plants.

## The eIF4E1/CERES and eIF(iso)4E/CERES complexes do not include eIF4G or eIF(iso)4G

As shown above, CERES´ 4E-BS is critical for CERES/eIF4E binding. Since this motif also mediates the association of eIF4G to eIF4E, these data suggest that CERES could bind to the same amino acids and occupy a similar position as eIF4G isoforms during the interaction with eIF4Es. This might lead to a situation in which CERES and eIF4G isoforms are not found in complexes with eIF4Es at the same time.

To test this hypothesis *in vivo*, we expressed cYFP-eIF4G, CERES-Flag and HA-eIF4E1 in *N. benthamiana* leaves and we carried out a first CERES immunoprecipitation analysis with anti-Flag antibodies. As shown in Fig. 3c, we can observe a clear band corresponding to eIF4E1 but not to eIF4G in the eluate from CERES immunoprecipitations (IP: α-Flag). These data further demonstrate the observation that CERES interacts with eIF4E1 and suggest that eIF4G is not present in this complex. In order to demonstrate that the absence of eIF4G in this complex was not due to technical issues that may have prevented the observation of eIF4G in CERES immunoprecipitations, we investigated whether the expressed eIF4G was able to bind to the portion of eIF4E1 in the extract not bound to CERES. To do so, we subjected the remaining supernatant obtained from the previous immunoprecipitation (from which we had depleted most of the CERES/eIF4E1 complexes) to an eIF4E1 immunoprecipitation (IP: α-HA). Despite the fact that the amount of immunoprecipitated eIF4E1 was lower after this second assay, we still could detect a band corresponding to eIF4G, reinforcing our hypothesis that eIF4G is able to interact with the eIF4E1 non-associated with CERES. All these data suggest that eIF4E1 is able to form complexes either with eIF4G or with CERES but those complexes already containing CERES do not include eIF4G.

To analyse whether the interaction between CERES and eIF(iso)4E precludes the binding of the eIF(iso)4G to the complexes, we carried out a similar approach co-expressing cYFP-eIF(iso)4G, Flag-CERES and HA-eIF(iso)4E in *N. benthamiana* leaves (Fig. 3d). As in the previous case, only the eIF(iso)4E but not the eIF(iso)4G was co-immunoprecipitated with

CERES, despite the portion of eIF(iso)4E not bound to CERES was able to form a complex with eIF(iso)4G.

All these data suggest that CERES complexes with eIF4E1 or eIF(iso)4E do not include the eIF4G and eIF(iso)4G proteins.

## CERES modulates translation of a reporter mRNA *in vitro*

The majority of the reported metazoan eIF4E interacting proteins appear to be negative regulators of translation; therefore, to investigate if CERES could play a similar role in plants, we carried out *in vitro* translation assays of a reporter mRNA in WGE in the presence of either the full-length CERES or of the CERESΔ563-570 version, which is unable to bind the eIF4E isoforms. As stated above CERES remains highly insoluble when expressed in *E. coli*, which impaired the use of *E.coli*-produced protein to supplement the *in vitro* translation system. In order to bypass this technical problem, prior to the addition of the reporter mRNA, we used the WGE to translate either CERES or CERESΔ563-570 (Fig. 3e). After their independent translation for 60 min, the reporter (a capped *Firefly luciferase* (*Fluc*) mRNA) was added to both extracts and translated for 30 min, when Fluc activity (as a measure of Fluc translation) was quantified in each sample. As shown in Fig. 3f, both CERES versions were accumulated to similar levels during the experiments; however, compared to the translation achieved in the presence of CERESΔ563-570 (which is unable to bind eIF4E), translation of the *Fluc* mRNA was significantly increased when full-length CERES was assayed (Fig. 3g). This result highlights a role of CERES in translation and the importance of the eIF4E binding for this function. Surprisingly, instead of supporting a role of CERES as a negative eIF4E-dependent regulator of translation, this result suggests that CERES could act as a positive regulator of translation initiation.

## CERES co-sediments with translation initiation complexes on sucrose gradients

Following this observation, we rationalised that if CERES promotes translation initiation in plants, it could be part of translation initiation complexes. Thus, to test this hypothesis, we analysed the distribution of CERES throughout the different fractions of a sucrose gradient (Figs. 3h-j). To do so, plant cell extracts from Arabidopsis seedlings were fractionated over 10-50% sucrose gradients obtaining the corresponding polysome profiles (Fig. 3h). From these profiles, the fractions corresponding to the 40S, 60S and 80S peaks and some of the polysome-containing fractions were isolated and the presence of AteIF4E1 and AtCERES throughout the fractions was monitored by western-blot (Fig. 3i). As controls, total extracts from wild-type plants (Col-0) and *ceres-1* mutant were included. As shown in Fig. 3i, CERES was highly accumulated in the 40S fraction which is characterised by the high enrichment of the 18S rRNA (Fig. 3j). CERES´ accumulation gradually decreased along the 60S, the 80S and the heavier polysome fractions. This accumulation pattern is also observed for eIF4E1, demonstrating that CERES co-sediments with eIF4E1 and both are highly accumulated in the fractions containing the initiation complexes.

These data suggest that CERES co-sediments with translation initiation complexes in plants.

### CERES interacts with AteIF4A2 and mediates the formation of alternative eIF4F complexes

As established before, CERES is a modular protein that, in addition to the 4E-BS, contains an LRR domain that covers a large part of the protein. Since LRR domains are involved in protein-protein interaction and CERES seems to be part of translation initiation complexes, we decided to analyse whether CERES was able to associate to other translation initiation factors, such as the eIF4A. To test this hypothesis, we transiently expressed HA-CERES and AteIF4A2-Flag in *N. benthamiana* leaves and carried out the immunoprecipitation of eIF4A2. As shown in Fig. 4b, CERES specifically co-immunoprecipitated with eIF4A2, which indicates that CERES interacts with eIF4A *in planta*.

To further explore the eIF4A2/CERES interaction, we generated a construct *p35S:HA-CERES-508* to express *in planta* a truncated version of CERES that includes the first 508 aa, but lacks the last 89 aa that contain the 4E-BS (Fig. 4a). As shown in Fig. 4b, this truncated version also interacted with eIF4A2, suggesting that the 4E-BS is not required for the interaction between CERES and eIF4A2.

This result opened the possibility that CERES could assemble into a complex able to support the simultaneous binding of eIF4E and eIF4A. To test this possibility, we co-expressed different combinations of the proteins eIF4E1, CERES and eIF4A2 fused to different tags in *N. benthamiana* leaves and we performed eIF4A2 immunoprecipitation analyses. As shown in Fig. 4c, eIF4E1 only co-immunoprecipitates with eIF4A2 in the presence of CERES, but not in its absence, which suggests that CERES, in a similar way to eIF4G, acts as a scaffolding protein that brings together eIF4E1 and eIF4A2.

### CERES interacts with AteIF3 and PABP *in vivo*

The previous results suggest that CERES recruits eIF4E and eIF4A *in vivo*. However, whether these complexes could promote translation in the absence of eIF4G isoforms was completely unclear. As cited above, apart from mRNA cap recognition (through its binding to eIF4E) and the loading of the eIF4A helicase, the other main function of eIF4G in translation is to facilitate the binding of the 40S ribosomal subunit to the mRNA. To accomplish this critical step, eIF4G interacts with the eIF3 complex and with the PABP (which allows and which stimulates, respectively, the binding of the 40S subunit) [31,32].

In order to test whether CERES could also promote this function we transiently expressed in *N. benthamiana* leaves HA-AtCERES and different subunits of the AteIF3 complex (eIF3e1, eIF3f and eIF3g1) fused to the Flag epitope to carry out eIF3 immunoprecipitation analyses. As shown in Fig. 4d, CERES specifically co-immunoprecipitated with all the eIF3 subunits assayed, although a stronger interaction was observed with eIF3f. Further co-immunoprecipitation analyses showed that the presence of CERES promotes eIF3f interaction with eIF4E1 (Fig. 4e), suggesting that, as in the case of eIF4A2, CERES acts as a molecular bridge able to support eIF3 binding to eIF4E containing complexes.

In addition, we also explored CERES interaction with PABP by co-immunoprecipitation analysis in *N. benthamiana* leaves. Among the different members of the PABP family, we selected PABP4, since this protein is ubiquitously expressed in plant tissues and its functional interaction with eIF4G and eIF(iso)4G2 during plant development has been

characterised in Arabidopsis [33]. As shown in Fig. 4f, this protein is specifically co-immunoprecipitated along with CERES, indicating that CERES also interacts with PABP *in planta*.

Finally, the interactions with the eIF4E1, eIF4A, eIF3d and eIF(iso)4E were also directly validated in Arabidopsis extracts (Fig. 4g). For this, we carried out co-immunoprecipitation assays (IP: α-HA) from extracts of seedlings from Col-0 or from a transgenic line that expressed HA-CERES under the control of a *35S* promoter. As shown in Fig. 4g, the endogenous (untagged) AteIF4E1, AteIF4A, AteIF3d and AteIFiso4E were specifically immunoprecipated along with CERES, further validating its interactions with these proteins in Arabidopsis.

All these data suggest that CERES is able to bind to the same critical translation initiation factors as eIF4G *in planta*.

## *ceres* mutants seem to show a reduction in protein translation at ZT5 but not at ZT0

The described results suggest that CERES could be involved in supporting mRNA translation initiation in plants. It has been previously reported that translation is regulated during the light/dark cycle. During this cycle ribosome loading rapidly decreases at night, reaching a minimum at dawn, and increases during the first hours of light from ZT2 to ZT6 [19,21]. Based on these differences, we decided to analyse whether CERES could specifically modulate translation in any of these two translational stages (Fig. 5). To do so, we carried out polysome profile analyses in seedlings from Col-0 and in both *ceres* mutants at ZT0 and ZT5 (in this latter case, when polysomal loading is at its highest level or close to it [19,21]). As shown in Fig. 5a, *ceres* mutants did not exhibit a clear alteration in their polysome profiles compared to the wild type at ZT0. However, at ZT5 (Fig. 5b), both *ceres* lines showed a clear reduction of polysome content and a concomitant increase in 80S monosomes (displaying a reduced polysomal / monosome ratio), which is a typical feature of treatments and mutants that show an inhibition in translation initiation.

Since both independent *ceres* mutants show a similar phenotype, and the analysis of two independent T-DNA alleles in the same gene is an accepted procedure to confirm the phenotype is caused by a specific gene disruption [34,35], our results suggest that CERES could support translation initiation in plants at specific stages of the diel cycle.

## Translation modulation by CERES impinges especially on certain set of mRNAs

To further analyse the possible function of CERES and to identify those mRNAs especially susceptible or recalcitrant to the general inhibition imposed on *ceres* mutants, we performed a super-resolution ribosome profiling experiment. To do so, we generated libraries from ribosome footprints (RFPs) and total RNA from three independent replicates of seedlings from Col-0, *ceres-1* and *ceres-2* that were collected at ZT5, and equimolecular amounts of each library were subjected to massive sequencing. As shown in Extended Data Fig. 6a, we obtained an excellent correlation among the RFP replicates and total RNA replicates, respectively (showing, in both cases, Pearson correlation factors between 0.98 and 1). The analysis of the total RNA and RFP fragments indicated that, in contrast to the large variations in the length of the fragments derived from the total RNA libraries, RFP

fragments showed a distribution that ranged from 22 to 32 nucleotides (nt) with a maximum at 28 nt (Fig. 6a). These fragments (28 nt) covered up to the 12$^{th}$ nucleotide upstream of the ATG and the last footprints covered the 15$^{th}$ nucleotide upstream of the stop codon (Fig.6b). These results are fully consistent with the average size of the ribosomal footprints and the position of the ribosome A-site and P-site described in Arabidopsis [36–38]. As expected, these sequences displayed an extraordinary enrichment of footprints in the same reading frame (Fig. 6b) with the majority of the footprints mapping to the CDS (73% in each genotype) and a sharp decrease in footprints along the 5´and 3´UTR sequences (Extended Data Fig. 6b). High periodicity was also obtained for the fragments ranging from 24 to 30 nt (Extended Data Fig. 7), and so these reads were used for further analyses. All these data demonstrated that RFP preparation and analysis were robust.

To gain insight into the function of CERES in gene expression, we firstly analysed the effect of CERES on the transcriptional output. To do so, we carried out a differential analysis of total RNA accumulation per gene in Col-0 and in both *ceres* mutants (Fig. 6c, upper panels). This analysis indicated that the number of genes significantly altered at the transcriptional level (absolute total RNA fold change values of $\log_2 \geq |0.58|$; padj $\leq 0.05$ in *ceres* mutants compared to Col-0) is extremely low: 6 and 26 genes in *ceres-1* and *ceres-2*, respectively, with only 4 genes showing an alteration at the transcript level in both mutants (Supplementary Table 2). As expected, one of the genes whose transcription was significantly reduced in both mutants was *CERES* (Fig. 6c, upper panels and Supplementary Table 2). This result suggests that the changes in polysome profiles observed in *ceres* mutants (Fig. 5b) are not correlated to general changes in transcript levels.

Additionally, we also carried out the analysis of the RFPs (Fig. 6c, lower panels). In this case, the number of genes with a significant alteration at the RFP level (absolute RFP fold change values of $\log_2 \geq |0.58|$; padj $\leq 0.05$ in *ceres* mutants compared to Col-0) was highly increased to 49 in *ceres-1* and 147 in *ceres-2* mutants (Supplementary Table 3). In order to identify possible physiological processes affected in the mutants, we carried out a GO analysis of the genes significantly altered at the RFP level in each mutant compared to the wild type. This analysis indicated that these sets are enriched in common functional categories such as response to light, response to radiation or response to carbohydrate, among others (Fig. 6d). The cited categories were also enriched, although with a lesser number of genes, when only the 20 common genes significantly altered at the RFP level in both mutants were analysed (Supplementary Table 3). A closer look to the reads in the RFP and total RNA sets allowed the identification of 8 genes that showed a distinct accumulation of reads in RFPs in *ceres* mutants that was not correlated with changes at the total RNA level, indicating that these genes are regulated at the translational level (Extended Data Fig. 8). These genes encode At5g23060, a calcium sensing receptor that controls the photosynthetic electron transport [39]; At3g56160, a member of sodium bile acid symporter family whose close orthologue BAS6 plays a main role in photorespiratory metabolism in Arabidopsis [40]; or At5g10180, a transporter involved in the maintenance of the sulphate status and the thiol levels [41]. In addition, two different desaturases FAD2 (At3g12120), a light induced enzyme involved in the synthesis of 18:2 fatty acids [42], and the sphingolipid desaturase 1 (SLD1, At3g61580) [43] were also observed.

In order to identify other possible translationally regulated genes in *ceres* mutants, we also carried out the analysis of translational efficiency (TE). This analysis, which included the information of total RNA and the RFP for each gene and used a different statistical model comparison, allowed the additional identification of the glucose transporter *VGT1* (At3g03090) [44] as a translationally regulated gene in both *ceres* mutants compared to Col-0 (Extended Data Fig. 8) (TE fold change -0.779 and -0.829 p-adj 0.017 and 0.049 in *ceres-1* and *ceres-2*, respectively, compared to Col-0).

All together these results suggest that translation modulation by CERES impinges especially on certain set of mRNAs and that some of them are involved in the light response and carbohydrate management.

### *ceres* mutants show a hypersensitive phenotype in response to glucose

Sugar production is a process intimately linked to the light/dark cycle that has been reported to peak around ZT5 [21]. As cited above, one of the functional groups regulated at the RFP level in *ceres-1* and *ceres-2* mutants compared to Col-0 is “response to carbohydrate stimulus”. Furthermore, one of the most highly downregulated genes in TE in both mutants is *AtVGT1* (Extended Data Fig. 8), a well-known glucose transporter whose mutants are characterised by a reduction in seed germination [44]. Based on these data, we decided to analyse the response to glucose in our mutants. To do so, we carried out germination assays in the presence of glucose. As shown in Figs. 7a-b, compared to the wild-type genotype, both *ceres* mutants showed a moderate developmental delay upon treatment with 6% glucose, displaying a reduction in the number of seedlings with green and expanded cotyledons (Fig. 7c). In order to discard that this phenotype was associated to the osmotic effect exerted by the glucose concentration, similar experiments were also carried out in the presence of 300 mM mannitol. In this case, no significant differences in germination or growth were observed between *ceres* mutants and Col-0 (Extended Data Fig. 9). These results suggest that CERES, most probably through the global drop in polysome loading at ZT5 and the altered translation of genes involved in carbohydrate response, modulates glucose management in plants.

## Discussion

Due to the importance of translation regulation through eIF4E-dependent mechanisms in other eukaryotes, there have been multiple attempts to identify possible eIF4E-dependent translational regulators in plants. These analyses included previous yeast two-hybrid screenings using AteIF(iso)4E as bait and a cDNA library from etiolated seedlings and the identification by mass spectrometry of proteins able to bind to the cap structure from Arabidopsis cell cultures and wheat seeds [15,26,28]. Despite the fact that these assays allowed the identification of different proteins that bind eIF4E isoforms in plants [26,27,29,30]; the direct role of these proteins in translation has remained mainly elusive. In this article we have identified CERES by a yeast two-hybrid screening using a complex cDNA library obtained from 14-day-old seedlings grown under control conditions and subjected to different stresses. CERES is a novel eIF4E-binding protein that shows a quite unconventional structure (formed by an LRR domain and a 4E-BS) that differs from the one

displayed by the eIF4G isoforms and from other eIF4E interacting proteins described before. Until date, most of the reported translational regulators that bind to eIF4E are negative regulators of translation [6–12]; however, the data presented in this article suggest that CERES acts as a plant-specific translation initiation factor that, through its binding to eIF4E and other translation initiation factors, boosts general translation and regulates the translation of subsets of mRNAs at specific stages of the diel cycle.

In addition to CERES, plants show other unique translation initiation factors, such as eIF(iso)4E and eIF(iso)4G, that seem to have evolved to allow plants to adapt translation to their special characteristics and needs [45–48]. One of these plant-specific characteristics is their immobile nature, which force them to adapt to the changing environmental conditions. In this article, we have defined the molecular role of CERES and we have analysed its role in translation at ZT5. During this specific stage of the diel cycle, CERES seems to participate in adapting translation to the sugar/energy status of the plant (which reaches its maximum level in this time-frame). In contrast, no difference was observed in our tested conditions in terms of lateral root emergence and main root length between *ceres* mutants and the wild-type genotype in response to phosphate starvation, paraquat treatment and high NaCl (data not shown). Despite this observation, a possible role of CERES in other plant-specific transitions or in response to other single or combined environmental cues should not be directly ruled out. In addition, it is also possible that, as it happens with the single mutants of the components of the eIF4F isoforms [49–51], the role of CERES in other plant physiological or developmental processes could be more clearly observed in combination with other mutants in genes coding for canonical translation initiation factors[46,52]. In this sense, this study provides evidence of the molecular role of CERES in translation and opens the possibility to analyse in the future other putative physiological roles of this novel and exciting translational regulator in plants.

## CERES is a non-canonical translation initiation factor with functional analogy to eIF4G

Our data indicate that CERES serves as a scaffolding protein able to coordinate, in a reminiscent way of eIF4G but in its absence, the assembly of translation initiation complexes in plants. In Arabidopsis, the eIF4G and eIF(iso)4G factors contain three well conserved modules that are involved in the recruitment of the translation initiation complexes: the 4E-BS (which mediates their interaction with eIF4E), the HEAT domain known as MIF4G (which in mammals mediates the binding with eIF4A, eIF3 and RNA) and the HEAT2/MA3 (which in mammals constitutes a second binding site for eIF4A) [1]. Instead, CERES shows a C-terminal 4E-BS and an LRR domain that covers a large portion of the N-terminal and central part of the molecule.

LRR proteins are involved in multiple functions related to development, physiological processes and defence response in plants. It has been widely reported that LRR genes that play a role in the two first processes are usually under a tight evolutionary pressure, reducing drift across orthologues, while proteins involved in defence are under strong diversifying selection, which leads to multiple copies of genomic loci, highly divergent sequences, duplications and re-arrangements [53]. As stated before, *CERES* is a single-copy gene in Arabidopsis with close orthologues in other plant species, which is in accordance with its

proposed role as a regulator of a main physiological process such as translation, widening the role of LRR proteins in this kingdom.

CERES orthologues show a high conservation of the 4E-BS and the LRR domains, which indicates that these domains may mediate protein-protein interactions, probably with conserved factors which are essential for its function. Accordingly, our results show that CERES interacts *in vivo* with eIF4A and with different subunits of the eIF3 complex while it retains the simultaneous binding to eIF4E. These data suggest that CERES, through its multiple interactions with translation initiation factors, act as a scaffolding protein able to recruit (as the canonical eIF4G) the 40S subunit of the ribosome to the cap structure and to drive translation. This hypothesis is reinforced *in vitro* by the analysis of translation in WGE and *in vivo* by the analysis of the polysomal profiles. Altogether, our results suggest that CERES is part of an alternative non-canonical translation initiation complex that contributes (most probably along with eIF4F complexes) to regulate translation initiation in plants.

Until now, most of the eukaryotic eIF4E interacting proteins with a 4E-BS repress either general or specific mRNA translation initiation due to their ability to inhibit the formation of the eIF4F complex [6–12,54]. An exception to this general rule is Mextli (Mxt), an eF4E interacting protein which promotes translation and is involved in stem cell maintenance in *Drosophila melanogaster*. Despite Mxt is not evolutionary related to eIF4G, it conserves two essential domains for eIF4G function: a canonical 4E-BS and an MIF4G domain. In such a way, Mxt binds to eIF4E, but bypasses the need of eIF4G through recruiting eIF3 [25]. As cited above, CERES lacks the MIF4G domain, which suggests that through evolution plants have conserved the 4E-BS to modulate eIF4E dependent translation, but they may have evolved a different structure to support eIF3 and eIF4A binding. Nevertheless, the discovery of CERES and Mxt opens the possibility of the existence of a divergent evolution of non-canonical translation initiation factors that, through the simultaneous binding of eIF4E and eIF3, govern translation and gene expression during specialised processes in eukaryotes.

### Does CERES compete with eIF4G for binding to eIF4E?

In our hands, any attempt to carry out competition analysis *in vitro* using *E. coli* purified recombinant proteins turned out to be unsuccessful since both the full length and the truncated versions of CERES remain highly insoluble when they are expressed in *E. coli.* This could be due to the structure of CERES, which contains multiple LRRs that should be finely folded to accomplish the native conformation, possibly making it too complex to achieve in *E. coli*. Similar problems were found when purifying AteIF4G. These technical problems abrogated direct translational competition assays *in vitro*. Despite these limitations, our data suggest that CERES interaction with eIF4E1 is quite strong since it supports the growth of co-transformants at high concentration of 3-AT in the yeast two-hybrid assays. In addition, it is also important to note that we detect eIF4E1/CERES complexes when CERES is expressed in the absence of ectopic eIF4E in *N. benthamiana* leaves (data not shown) or in Arabidopsis (Fig. 5g). These data suggest that CERES may compete with eIF4G for eIF4E binding. Alternatively, it is also possible, and a more likely scenario, that, in contrast to the situation in mammals where eIF4E is a rate limiting factor [55], eIF4E is not so limiting in Arabidopsis and that, therefore, a proportion of eIF4E could

be free from the eIF4F complexes to interact with CERES. In any case, the analysis of polysome profiling suggests that CERES is not exclusively in its own in charge of the general translation at ZT5, since translation is not completely inhibited in *ceres* mutants. This result favours the co-existence of canonical translation initiation complexes with CERES-containing complexes that could coordinately support translation initiation under specific conditions.

## CERES seems to regulate translation at ZT5

The daily alteration between light and darkness is one of the most prevailing environmental changes experienced by plants. During these cycles plants dynamically adjust their growth and metabolism to the light and energy conditions [21]. These rearrangements are driven by massive and subtle changes in gene expression that are orchestrated at different levels that include transcription and translation. It is well known that translation activity tightly correlates with light sensing and cellular sugar levels in plants [19–21]. However, with very few exceptions, the mechanisms involved in this regulation are quite unknown. One of these few exceptions is target of rapamycin (TOR), a kinase that coordinates protein synthesis with cellular energy/nutrient availability in different eukaryotes [56,57]. In plants, inactivation of this master kinase promotes a decrease in polysome accumulation, demonstrating its role in translation [57,58]. TOR phosphorylates different substrates involved in translational regulation in plants. This is the case of the S6K1, a regulator of the 40S ribosomal protein S6 (RPS6) [59], and the MA3 domain-containing translation regulatory factors (MRF proteins). These latter proteins bind to eIF4A and promote translation during energy-deficient conditions, especially during dark and starvation [60]. These data suggest that plants have evolved common and specific mechanisms (that include MRFs and CERES) to control translation and, through this process, to accomplish cellular adaptation to the specific nutritional and energy status of the organism.

In this article we provide two different and complementary pieces of evidence of the role of CERES in the regulation of translation during the diurnal cycle. On the one hand, our polysomal profile analyses show that CERES promotes general translation at ZT5, when translation and energy status is at the maximum level, but has no apparent impact during dawn (when the translational and energy level is at minimum). Additionally, the analysis of our super-resolution ribosome profiling at ZT5 suggests that, during this stage, CERES modulates the expression at the RFP level of mRNAs involved in cellular processes related with plant response to light and response to carbohydrates. These data suggest that CERES, through its interaction to eIF4E and the formation of alternative initiation complexes, is involved in boosting overall translation and in modulating the specific translation of mRNAs related to light and carbohydrate response when the translational demand and carbon supply are at their highest level.

The data presented in this article suggest that during evolution, different eIF4E interacting proteins have evolved divergently in a way that, through the regulation of eIF4E, are able to adjust translation to the nutritional and metabolic conditions of the organism. It has been proposed that 4E-BPs emerged early in eukaryotic evolution to act as metabolic “brakes” and shut down cap dependent translation in response to nutritional shortage and

environmental stresses [5]. Our results indicate that CERES integrates the nutritional stimuli and likely regulates some aspects of translation in plants, but, instead of inhibiting translation when conditions are not favourable (as in the case of the 4E-BPs in metazoans), CERES seems to boost general translation and modulate translation of different mRNA subsets when the energy and carbon supply is high.

## Materials and Methods

### Plant Material and growth conditions

Arabidopsis T-DNA insertion mutants *ceres-1* (SALKseq_129709) and *ceres-2* (SALKseq_054336) were acquired from the Arabidopsis Biological Resource Center (ABRC) [61]. *Arabidopsis thaliana* ecotype Columbia-0 (Col-0) was used as wild-type genetic-background control. Unless otherwise stated, all seeds were surface sterilised, stratified at 4°C for 48 h and grown at 22°C using a 16 h light photoperiod. For growth on plates, Murashige and Skoog (MS) medium supplemented with 1% (w/v) sucrose was used in all cases unless otherwise stated.

### Constructs and molecular cloning

To obtain the *pCERES*:*CERES-GFP* constructs, a genomic fragment expanding from -1700 to +3022 bp position of *CERES* gene was cloned into the Gateway Binary Vectors pMDC107 [62]. The constructs *p35S:Flag-(CERES, eIF4E1* and *eIF(iso)4E*), *p35S-HA-*(*CERES, CERES*$^{Y563A}$*, CERESΔ563-570*, *eIF4E1* and *eIF(iso)4E*), *p35S:(eIF4A2, eIF3e1, eIF3f and eIFg1)-Flag*, *p35S:PABP4-HA*, *p35S:RFP-eIF4E1*, *p35S:cYFP-*(*eIF4G* and *eIF(iso)4G*), *p35S:Ω sequence-HA-CERES* were obtained by cloning the gene CDSs in frame with the corresponding epitopes in the binary vectors pGWB12, pGWB15, pGWB11, pGWB14 [63], pGWB655 [64], pBiFP3 (Parcy CNRS Grenoble) and pGWB402omega [65], respectively, using the Gateway cloning system (Life Technologies). In the case of eIF4A2, eIF3e1, eIF3f, eIF3g1 and PABP4, the corresponding clones derived from S. Dinesh-Kumar ´s laboratory were used for gene CDS amplification. These clones were obtained from the Arabidopsis Biological Resource Centre.

Constructs for the two-hybrid analyses were generated by cloning the cDNA fragments coding for eIF4E1, eIF(iso)4E, CERES and eIF4G into *pDONR207*. Gene fusions to *Gal4-AD* or *Gal4-BD* were obtained by recombination between their corresponding *pDONR* vectors and *pDEST-GBKT7* and *pDEST-GADT7* [66].

### Site-Directed Mutagenesis

PCR-based site mutagenesis was performed as described in [67] using as template the amplified coding sequence of *CERES* in the pDONR207 vector. The primers used for the mutagenesis are included in Supplementary Table 1.

### qRT-PCR analysis

RNA was isolated from 7-day-old seedlings or from different tissues of 10-day-old seedlings and 4-week-old plants. qRT-PCR analysis was carried out as described in [68], using either *ACT2* (At3g18780) or *UBC* (At5g25760) for normalisation. Each experiment was

conducted in three technical replicates with three biological replicates. Primer sequences are listed in Supplementary Table 1.

### Co-immunoprecipitations in *N. benthamiana* leaves

Co-immunoprecipitation analyses were carried out as described in [69,70]. In all cases the assays were repeated at least three times obtaining similar results.

### Western-blot analysis and antibodies

Proteins were separated by SDS-polyacrylamide gel electrophoresis, blotted to nitrocellulose membranes and analysed with specific antibodies against HA (Roche), Flag (Sigma Aldrich), GST (Santa Cruz Biology), GFP (Roche), RFP (5F8, Chromotek), Myc (Clone 4A6, Merck), eIF4A (St. John's laboratory), eIF3D (sc-28856, Santa Cruz), AteIF4E and AteIF(iso)4E (kindly provided by Dr. J. L. Gallois, INRA, France) and TaeIF4E (kindly provided by Dr. Karen Browning, University of Texas, USA).

The C-terminal part of CERES (base pairs 1471-1794) was cloned into pDEST17 vector (Invitrogen) and transformed into *E. coli* strain BL21. Cells were induced for protein expression by adding 0.1 mM IPTG and the proteins were separated by SDS-polyacrylamide gel electrophoresis. Following SDS-PAGE, the gels were incubated in cold 2 M KCl until the protein bands became opaque. The band corresponding to Ct-CERES was excised from the gel. This band was used to immunise rabbits for antiserum production by Pineda Antibody Services (Germany).

### Yeast two-hybrid screening and directed two-hybrid analyses

For yeast two-hybrid screening, the *pDEST-GBKT7-eIF4E1* plasmid was transformed into the Y187 strain. After testing for absence of toxicity and transcriptional activation, this transformed strain was co-cultivated with an Arabidopsis cDNA library pre-transformed into the strain AH109. This library was obtained from a mix of cDNAs from 14-day-old seedlings grown under control conditions or subjected to different stresses (4°C, 42°C, 150 mM NaCl, 400 mM sorbitol, 300 μE/m2/sec, darkness, 10 mM paraquat and 20 mM $H_2O_2$) for 60 and 120 min. The mated clones were initially screened on SD/–Leu/–Trp/–His/+10 mM 3-AT and the positive clones were further selected on SD/–Leu/–Trp/–His/+60 mM 3-AT. Identification of the eIF4E1 interactors was done by amplification and sequencing of the DNA contained in the prey vector and subsequent BLAST analysis against Arabidopsis annotated genes (https://www.arabidopsis.org/Blast/index.jsp).

Directed yeast two-hybrid analyses were carried out as described in [71].

### Microscopy analyses

Co-localisation analyses were carried out by transient expression of *pCERES:CERES-GFP* and *p35S:RFP-eIF4E1* constructs in 3-week-old *N. benthamiana* leaves. Plant tissue was imaged 3 days post-agroinfiltration using a Leica SP8 confocal microscope (Leica Microsystems) with an Argon ion laser. GFP was excited at 488 nm and the emitted light was captured at 495-520 nm. RFP was excited using 561 nm and emitted light captured at 590-630 nm. Sequential scanning was used to image GFP and RFP as described in [72].




Europe PMC Funders Author Manuscripts

Experiments were done at least three times, obtaining similar results. A representative replicate is shown in the figures.

### *In vitro* transcription and translation

*In vitro* transcription was carried out with the MEGAscript™ Kit (Thermo Fisher) following manufacturer's instructions. For *CERES* and *CERESΔ563-570* mRNA synthesis, PCR products that contained the T7-promoter and -terminator were amplified from the *pGBKT7-CERES* or *pGBKT7-CERESΔ563-570* vectors. To obtain the *Luciferase* mRNA we performed a PCR to introduce the T7 promoter sequence using *pcDNA-Luciferase* as template. mRNAs were capped using Vaccinia Capping System (New England Biolabs).

*In vitro* translation was done using the Wheat Germ Extract (WGE) system (Promega). Luciferase activity was measured using 5 μL of *in vitro* translation reaction as described in manufacturer's protocol. Statistical analysis was performed with GraphPad Prism Software (GraphPad Software Inc.).

### Polysome profiling

9-day-old seedlings were harvested at Zeitgeber time 0 (ZT0, immediately before the lights turned on) and at Zeitgeber time 5 (ZT5, 5 h after the lights turned on) and were immediately frozen in liquid nitrogen. 700 mg of frozen tissue was pulverised in liquid nitrogen with a mortar and pestle and thawed in 800 μL of ice-cold polysome extraction buffer (160 mM Tris-HCl [pH 8.4], 80 mM KCl, 40 mM $MgCl_2$, 5.6 mM EGTA, 4% (v/v) TritonX-100, 50 μg/mL chloramphenicol, 80 μg/mL cycloheximide, 200 mM sucrose) in a rotary shaker for 15 min at 4ºC. The raw extract was clarified by centrifugation at 13,000 *g* for 30 min at 4 °C. The supernatants were layered on top of a 12.5 mL 10%-50% sucrose density gradient (containing 40 mM Tris-HCl [pH 8.4], 20 mM KCl, 10 mM $MgCl_2$, 15 μg/mL chloramphenicol, 10 μg/mL cycloheximide) and centrifuged at 39,000 rpm for 2.5 h at 4 °C in a SW40 rotor. After ultracentrifugation, the gradient was monitored at $A_{256}$ while being fractionated into 600 μL fractions using a density gradient fractionation system.

For RNA extraction of the different fractions, 0.5% (w/v) SDS was added to 300 μL of each fraction prior to TRIZOL extraction following the manufacturer's instructions. For protein extraction, 300 μL of the corresponding fractions were extracted by the chloroform–methanol method [73]. The protein pellets were resuspended in 100 μL of 1x Laemmli buffer and loaded on the gels for further analysis.

At least three biological replicates were performed for each analysis, showing similar results. Thus, a representative replicate is shown in the figures.

For gradient fraction quantification, three biological replicates from each genotype collected at ZT0 and ZT5 were subjected to polysome profiling analysis and, for each replicate, the area below the curve corresponding to free mRNA, 60S, 80S and polysomes was normalised by the total area of each gradient using ImageJ. Statistical analysis was performed with GraphPad Prism Software (GraphPad Software Inc.).

### 7-Methyl-GTP pull-down assays

Plant extracts (generated in co-immunoprecipitation buffer) were incubated with 50 μL of 7-methyl-GTP Sepharose® 4B GE Healthcare or Sepharose 4B (when stated) for 2 h at 4ºC. After washing, the retained proteins were eluted in 50 μL of 2x Laemmli buffer and subjected to SDS-PAGE. Experiments were done at least three times, obtaining similar results. Thus, a representative replicate is shown in the figures.

### Super-resolution ribosome profiling

Three independent biological replicates were used for the RFP (ribosomal footprint) and total RNA analysis. For each replicate, seedlings from Col-0, *ceres-1* and *ceres-2* were grown and collected at ZT5 as previously described. 200 mg of frozen tissue was thawed in 800 μL of plant lysis buffer (100 mM Tris-HCl [pH 8.0], 40 mM KCl, 20 mM $MgCl_2$, 2% (v/v) polyoxyethylene (10) tridecil ether, 1% (w/v) sodium deoxycholate, 1 mM DTT, 100 μg/mL cycloheximide and 10 U/mL DNAse I). The lysate was vortex-mixed until homogenised and incubated on ice for 10 min using a rocking shaker. Lysates were clarified at 20,000 *g* for 10 min at 4 °C. 100 μL of supernatant was used to extract total RNA and to generate the RNA-seq libraries. 200 μL of the supernatant was treated with 17.5 U of nuclease per 40 μg of RNA at 25ºC for 1 h to generate the RFP libraries. The nuclease was provided by the ARTseq/TruSeq Mammalian Ribo Profile Kit (Illumina). The rest of the steps to generate the libraries were performed according to the cited Illumina kit using size exclusion columns (Illustra MicroSpin S-400 HR Columns, GE Healthcare) and Zymo RNA clean and concentrator kit (Zymo Research). After cDNA circularisation the RFP and total RNA libraries were barcoded and amplified by 13 cycles and 9 cycles of PCR, respectively. PCR products were purified from acrylamide gels and the libraries were pooled for single-end 50-bp sequencing in a HiSeq 2500 sequencing platform.

### Super resolution ribosome profiling analysis

The raw data were firstly subjected to a quality control with FastQC. Afterwards, the adaptor sequence (AGATCGGAAGAGCACACGTCT) was removed using FASTX_clipper included in FASTX_toolkit [74]. Non-clipped reads were discarded for downstream analysis. After adaptor removal, the remaining reads were searched for expected contaminant RNA sequences in Arabidopsis, including rRNA, tRNA and ncRNA sequences, using Bowtie. The unmapped reads were then aligned to the Arabidopsis genome using TAIR10.33 reference and the split-aware aligner TOPHAT2 [75], version 2.1.0, allowing only unique alignments (i.e., each read was allowed to map to one location only) and not more than two nucleotide mismatches. To minimise errors from ambiguous read mappings, only the unique mapping results were used throughout this study.

Several steps of analysis and statistical presentation of the data were performed and plotted in R, version 3.5.1, using a combination of command-line software tools, R packages including ggplot2 [76], RiboProfiling [77], GenomicFeatures [78], riboSeqR [79], Rsamtools [80] and DESeq2 [81].

Trinucleotide periodicity and meta-gene analysis over start/stop codons of translating ribosomes (RFP) were determined using the riboSeqR with the transcriptome alignment

against the coding sequences of representative gene model (longest CDS in locus). Matches between 24 and 30 nucleotides were used for further analysis. Reads were assigned to genomic features (5′-UTR, CDS and 3′-UTR) with the RiboProfiling package using the aligned bam files.

Total RNA- and RFP-differentially expressed genes within the different data sets were identified using the R package DESeq2 that uses the negative binomial distribution to model the variations. Normalised read counts in CDS for Total RNA and RFP samples were used. For these analyses, the hypothesis testing was performed by a Wald test. Besides the genotype, batch was also considered as a covariate in the model.

Translation Efficiency (TE, RFP/ Total RNA ratio) was calculated using the likelihood ratio test (LRT) for full and reduced (without the interaction term) model comparison according to the pipeline described in systemPipeR Workflow for Ribo-Seq and polyRibo-Seq Experiments (https://pdfs.semanticscholar.org/2bb3/a1305835e7304d2cf5a5e788b08d00e025e6.pdf).

Differentially expressed genes (in Total RNA, RFP and TE) were defined as those with absolute fold change values of $\log_2 \geq |0.58|$; padj ≤0.05 in *ceres* mutants compared to Col-0. padj value corresponds to the p-value adjusted for multiple testing using Benjamini-Hochberg method.

### Other bioinformatics analysis

The identification of CERES orthologues was carried out using the Basic Local Alignment Search Tool (https://blast.ncbi.nlm.nih.gov/Blast.cgi). GO analysis was done using the topGO R package (Alexa A, Rahnenfuhrer J (2019). topGO: Enrichment Analysis for Gene Ontology. R package version 2.36.0) using the runTest function, the classic algorithm and the Fisher statistical test for the analysis of p-value. In this case, the p-values were unadjusted for multiple test comparisons. The genes upregulated and downregulated at the RFP level compared to Col-0 were pooled in the analysis of each mutant. The reference list included all the genes expressed, with more than 10 counts in each condition, at the Total RNA level.

### Phenotypic analysis in response to glucose and mannitol

*ceres* mutants were germinated and grown for 7 days side by side with the wild type in 0.5x MS agar in the absence of sucrose and glucose or supplemented with 6% (w/v) glucose or 300 mM mannitol. For quantitative analysis of the phenotype, the percentage of seedlings with fully expanded green cotyledons was calculated and plotted. n=8 independent experiments from three independent seed batches were analysed. Each replicate included 3 different plates of each treatment with 100 seeds per genotype. Statistical analysis was performed with GraphPad Prism (GraphPad Software Inc.).

## Extended Data

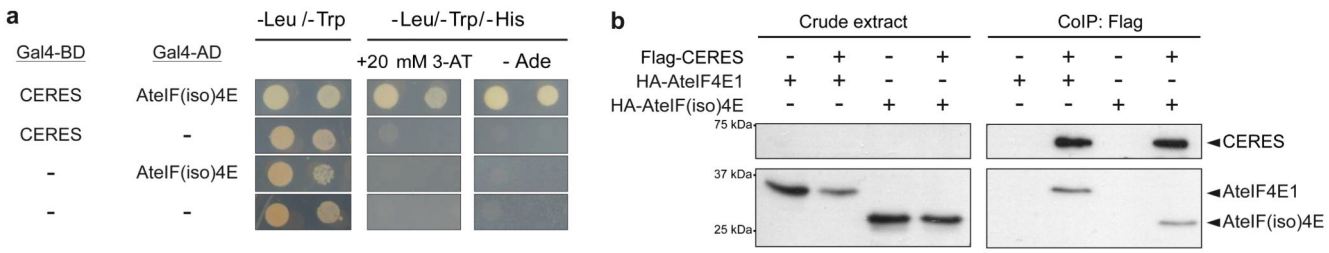


**Extended Data Fig. 1. CERES interacts with AteIF(iso)4E.**

(**a**) Yeast two-hybrid assays to analyse CERES interaction with AteIF(iso)4E. The proteins fused to the Gal4-BD and Gal4-AD that were co-expressed in the AH109 strain are shown on the left of the panel. Independent co-transformants were tested for growth in non-selective medium (-Leu-Trp) or prototrophy-selective medium (-Leu, -Trp, -His) in the presence of 3-AT or in the absence of Ade. The constructs expressing the bare Gal4-BD and Gal4-AD were used as controls (-). (**b**) CERES interacts with AteIF4E1 and At(iso)4E *in vivo*. Protein extracts (crude extracts) from *N. benthamiana* leaves transiently expressing, under the control of the *35S* promoter, different combinations of Flag-CERES, HA-AteIF4E1 and HA-AteIF(iso)4E were subjected to immunoprecipitation using anti-Flag beads. The presence of the different proteins in the crude extracts and in the eluted fractions from CERES immunoprecipitations (IP:α-Flag) was analysed by western-blot using anti-HA and anti-Flag antibodies. The experiments in (**a-b**) were repeated independently three times with similar results.




Europe PMC Funders Author Manuscripts

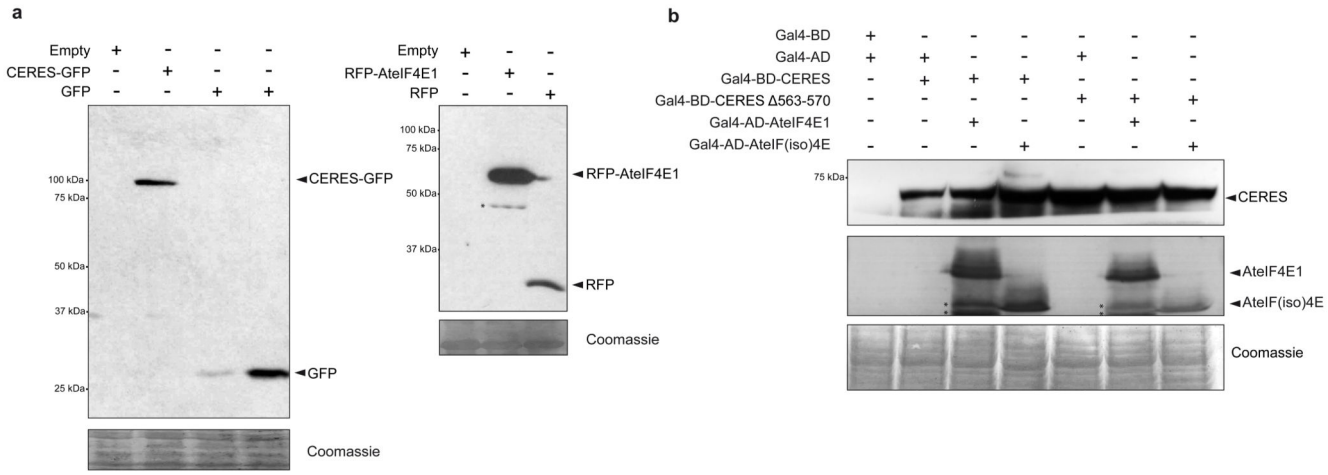


**Extended Data Fig. 2. Western-blot to analyse the size of the fusion proteins and the accumulation of the proteins of interest in Figure 1c and Figure 2d.**

(**a**) Western-blot of extracts from *N. benthamiana* leaves expressing the constructs *pCERES:CERES-GFP* or *p35S:GFP* (in this case two extracts with different expression level of GFP were included) (left panel) or the constructs *p35S:RFP* and *p35S:RFP-AteIF4E1* (right panel) using the anti-GFP and anti-RFP, respectively. The Coomassie staining is provided as loading control of the assay. (**b**) Western-blot of yeast extracts that expressed from the *pDEST-GADT7* and *pDEST-GBKT7* vectors the different proteins of interest. These vectors allow the fusion of the proteins to the Gal4-AD and the HA and to the Gal4-BD and the c-Myc epitopes, respectively. The fusion proteins were detected using the anti-HA and anti-Myc antibodies. Possible degradation products are marked by an asterisk. The experiments in (**a-b**) were repeated independently twice with similar results.




Europe PMC Funders Author Manuscripts

Europe PMC Funders Author Manuscripts

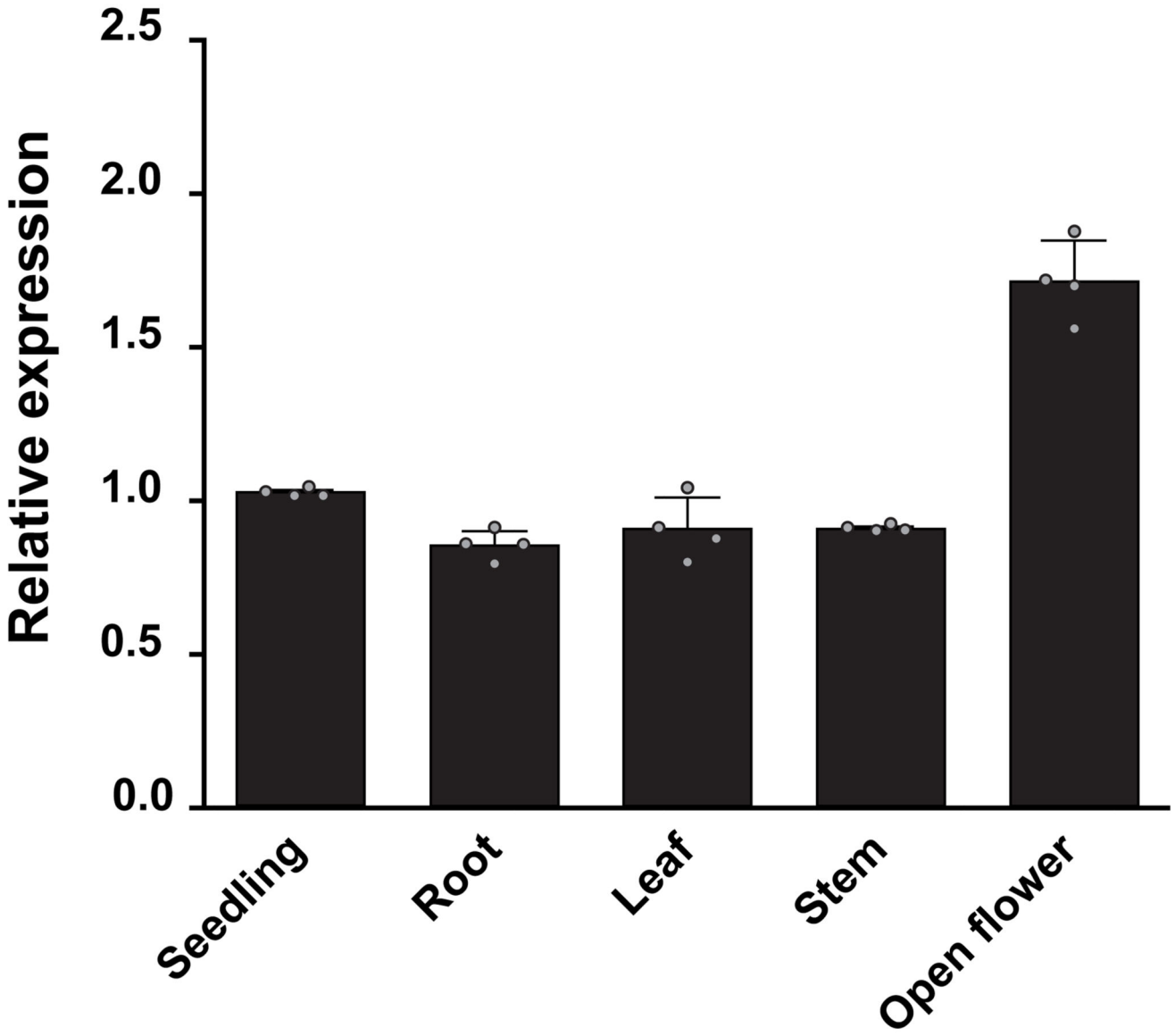


**Extended Data Fig. 3. Analysis of *CERES* expression by qRT-PCR in different Arabidopsis tissues.**

The relative expression of *CERES* mRNA was analysed in 7-day-old whole seedlings, 10-day-old roots and 4-week-old leaves, stems and open flowers. Fold change values, shown as means ± SD (n=4 independent experiments), are related to the expression in seedlings that was arbitrarily assigned value 1 after normalisation with the calibrator gene *UBC*.

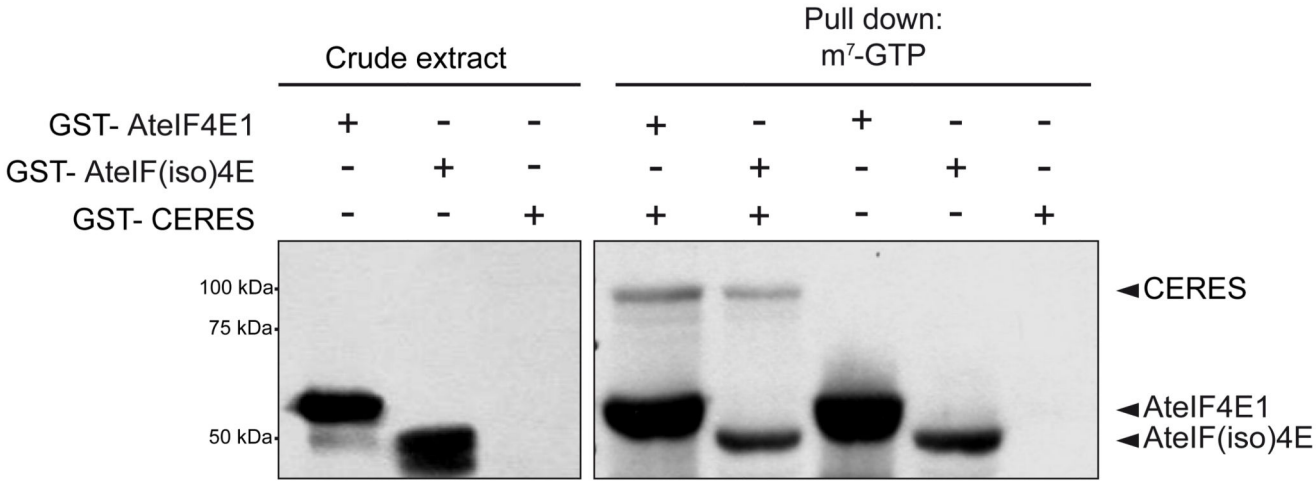


**Extended Data Fig. 4. CERES forms part of cap-binding complexes in vitro in the presence of AteIF4E1 and AteIF(iso)4E.**

Recombinant AteIF4E1, AteIF(iso)4E and CERES fused with GST were expressed in *E.coli* (crude extract). These extracts were combined as detailed in the figure (using in all cases a higher amount (8-fold) of recombinant CERES) and subjected to a 7-methyl-GTP chromatography. The corresponding eluates were analysed by western-blot using a commercial anti-GST antibody. This experiment was repeated independently twice with similar results.

Europe PMC Funders Author Manuscripts

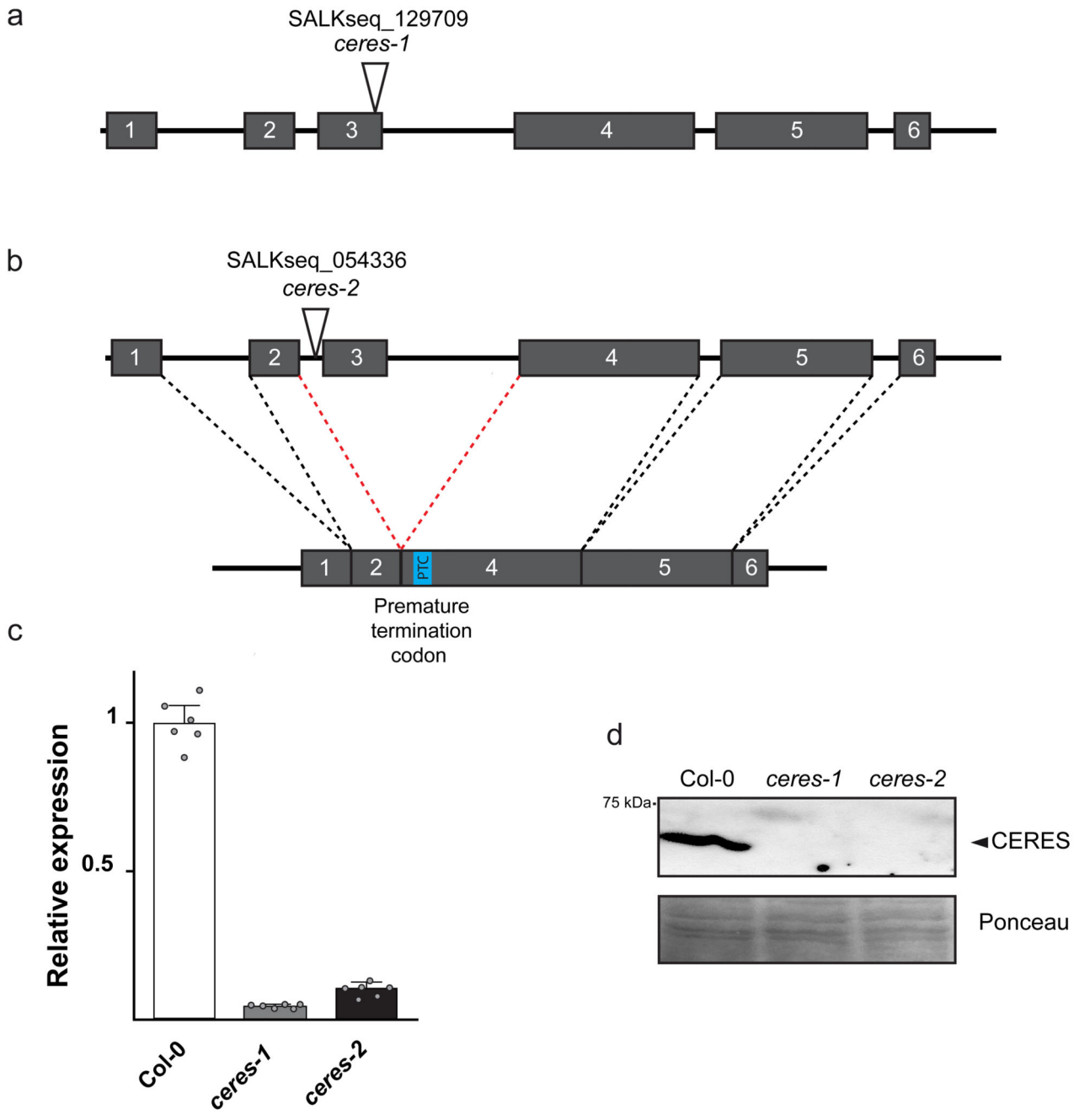


**Extended Data Fig. 5. Description of *ceres-1* and *ceres-2* mutants and expression analysis.**

(a-b) Schematic genomic organisation of *CERES.* Exons are indicated as rectangles. The triangles mark the position of the T-DNA insertions in the *ceres-1* (**a**) and *ceres-2* (**b**) mutants. (**b**) Schematic organisation of *CERES*´ CDS in *ceres-2.* This mutant shows an aberrant splicing event that introduces a premature stop codon (PTC) in its sequence. (**c**) Analysis of *CERES* expression in 15-day-old seedlings from Col-0, *ceres-1* and *ceres-2* by RT-qPCR. Expression values are shown as mean ± SEM from n=6 independent samples. These values are related to the value of Col-0 that was arbitrarily assigned value 1 after

normalization with the calibrator gene *ACT-2*. (**d**) Western-blot analysis of CERES accumulation in Col-0 and in *ceres* mutants using specific anti- CERES antibodies generated in the laboratory. The Ponceau staining of the membrane is provided as loading control. This experiment was repeated independently four times with similar results.



Europe PMC Funders Author Manuscripts

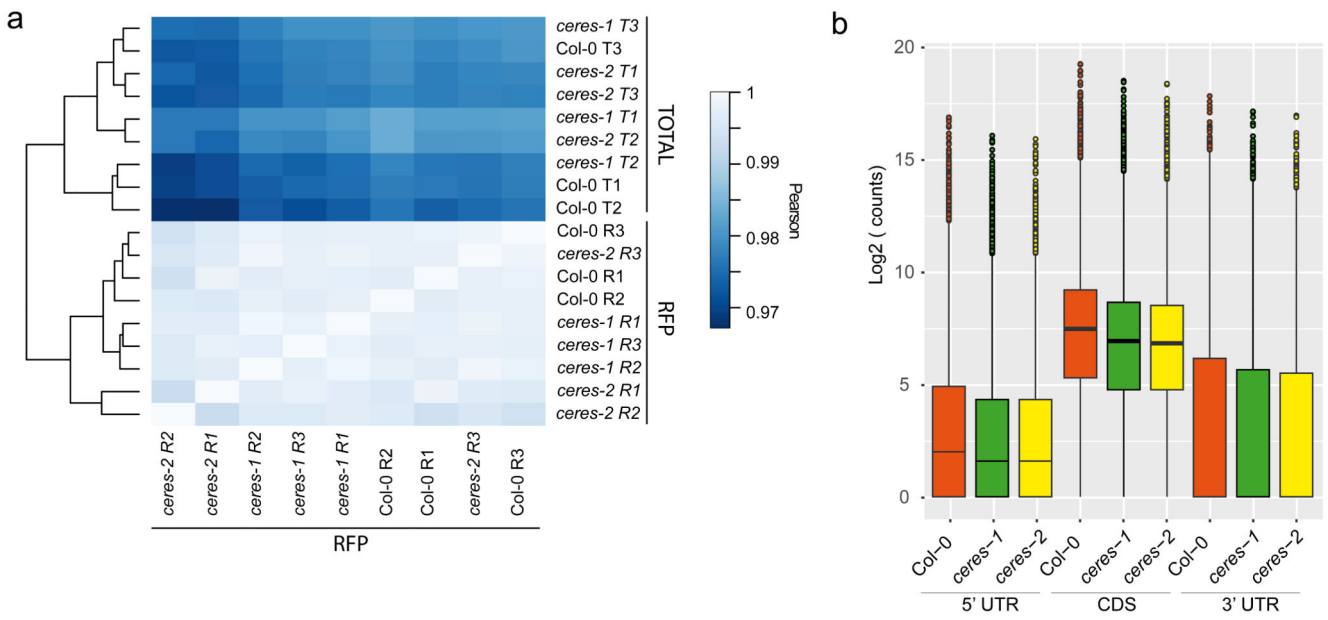


**Extended Data Fig. 6. Correlation and RFP coverage analyses.**

(**a**) Correlation plots of the RFP (R1, R2 and R3) and total RNA (T1, T2, T3) samples of each genotype used for the super-resolution ribosome profiling analysis. (**b**) Boxplots of RFP coverage on 5' UTR, CDS and 3' UTR regions. RFP reads from the replicates (n=3 independent experiments) were grouped for each genotype. The middle bars represent the median, while the bottom and top of each box represent the 25th and 75th percentiles, respectively, and the whiskers extend to 1.5 times the interquartile range. Dots are outliers. Median value for reads on 3'UTRs is 0.

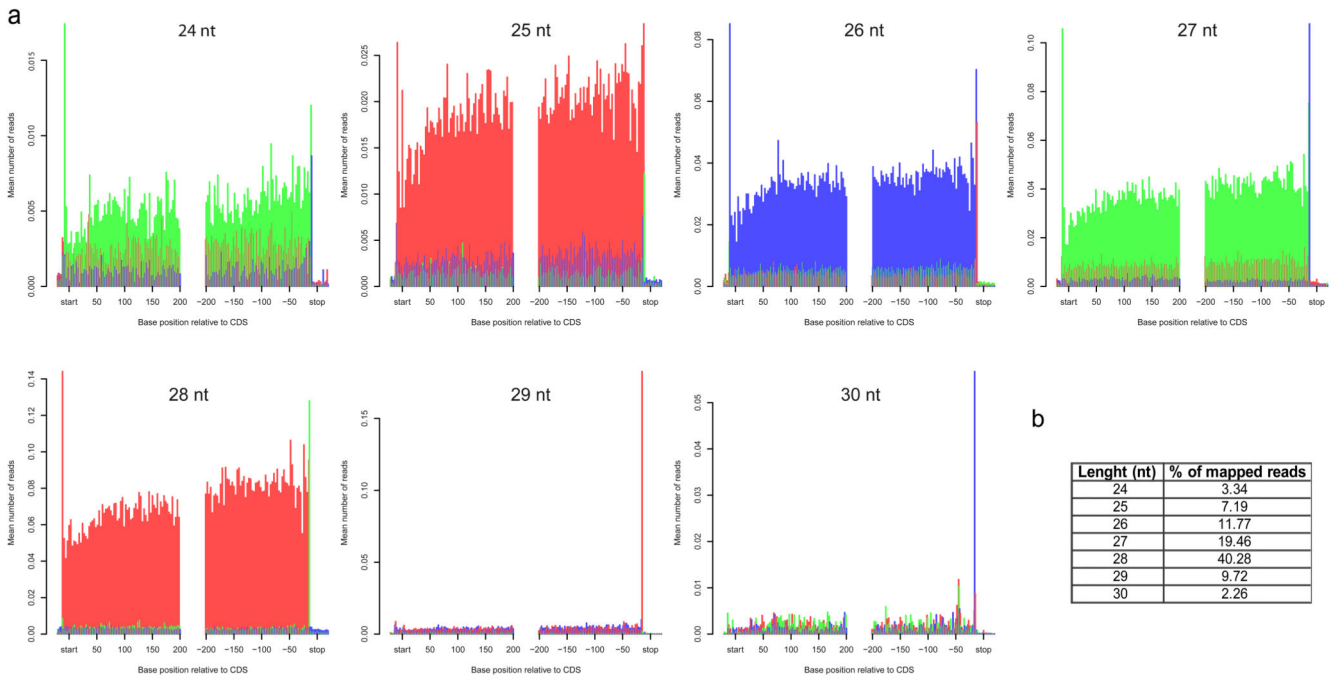


| Lenght (nt) | % of mapped reads |
|---|---|
| 24 | 3.34 |
| 25 | 7.19 |
| 26 | 11.77 |
| 27 | 19.46 |
| 28 | 40.28 |
| 29 | 9.72 |
| 30 | 2.26 |

**Extended Data Fig. 7. Periodicity analysis (cumulative plots) of RFP reads ranging from 24 to 30 nt in length.**

The first nucleotide of each footprint is used to represent its location on the transcript. The three reading frames are shown in red, blue and green. As representative data, the analysis of RFP from Col-0 replicate 1 is shown. (**b**) Percentage of RFP reads derived from the 24-30 nt fragments used in the study.




Europe PMC Funders Author Manuscripts

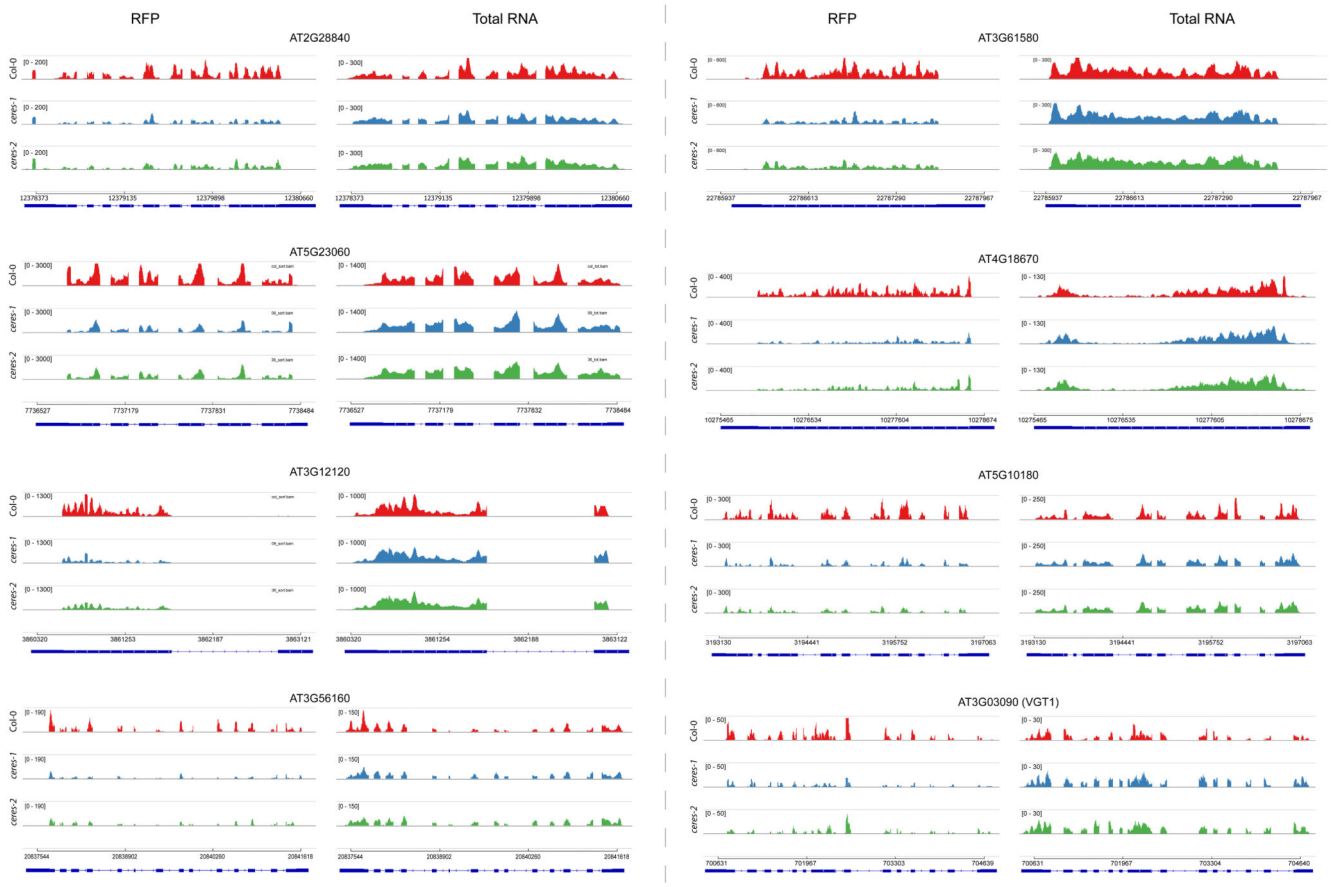


**Extended Data Fig. 8. Coverage of RFP and total RNA reads on selected genes in Col-0 and *ceres* mutants.**

The scale of the reads for each gene is indicated in the upper left. Based on the total RNA reads, the most prevalent predicted genomic organisation is shown in the bottom panel of each gene. Exons are indicated as dark blue rectangles and introns as dark blue lines. In this analysis the reads of each genotype from n=3 independent experiments were combined.




Europe PMC Funders Author Manuscripts

Europe PMC Funders Author Manuscripts

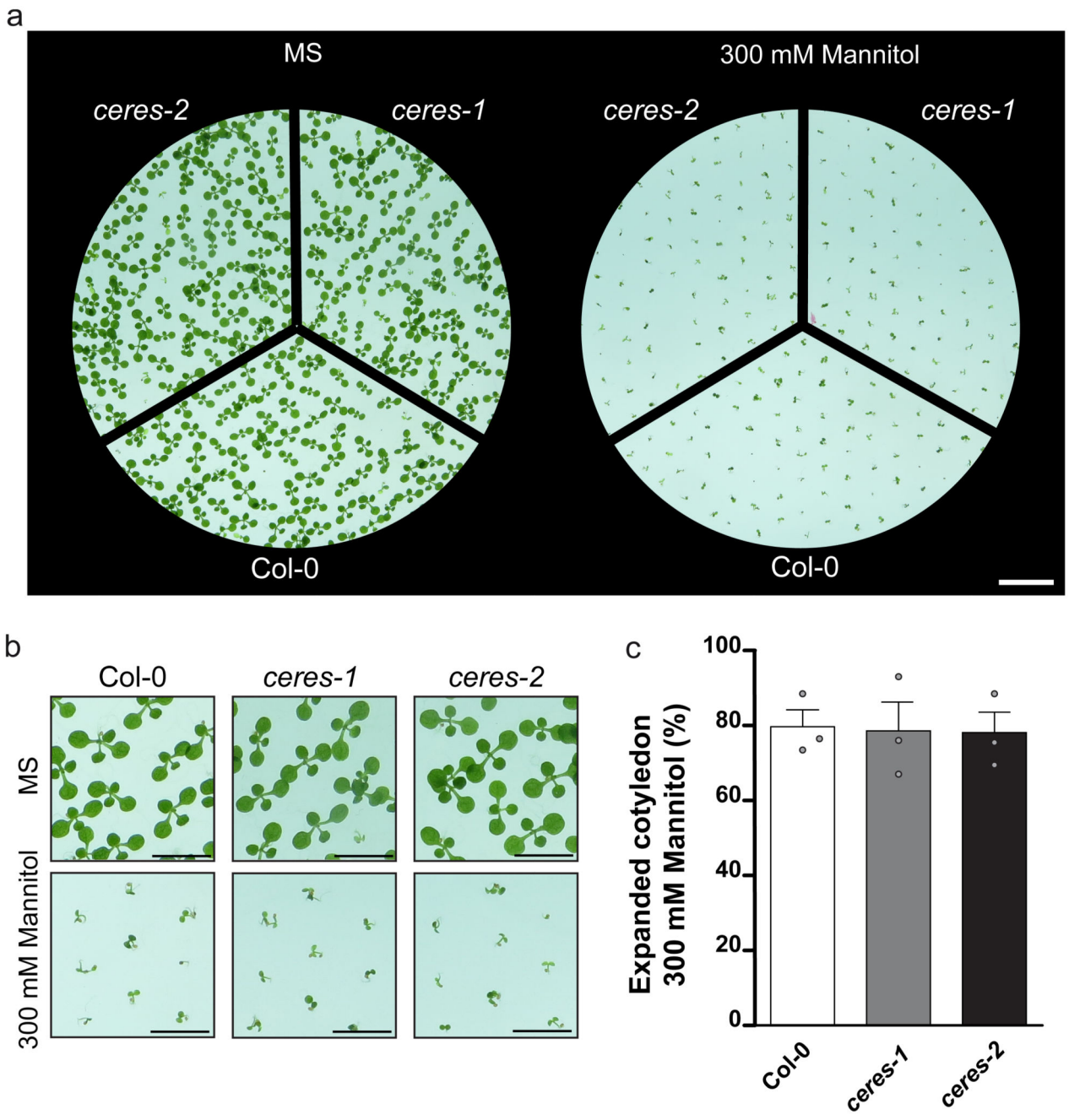


**Extended Data Fig. 9. *ceres* mutants do not seem to show an altered phenotype in response to mannitol.**

(**a**) Representative growth of Col-0, *ceres-1* and *ceres-2* seedlings in medium lacking mannitol (control) or supplemented with 300 mM mannitol for 7 days. (**b**) Close-up views of the upper panel. (c) Percentage of seedlings from Col-0, *ceres-1* and *ceres-2* that develop green and expanded cotyledon in the presence of mannitol. n=3 independent experiments were analysed. Values are shown as means ± SEM. No statistical difference between Col-0

and *ceres* mutants ($p < 0.05$) using one-way ANOVA analysis was observed. The scale bars in (**a**) and (**b**) correspond to 1.5 cm and 7.5 mm, respectively.

## Supplementary Material

Refer to Web version on PubMed Central for supplementary material.

## Acknowledgements

This research has received funding from the European Research Council under the European Union's Seventh Framework Programme (FP/2007-2013) / ERC Grant Agreement n. 260468 to M.M.C. and from the grant S2013-ABI2748 from CAM. In addition, this work has been partially financial supported by RTI2018-095946-B100 from MICIU and by. "Severo Ochoa Programme for Centres of Excellence in R&D" from the Agencia Estatal de Investigación of Spain (grant SEV-2016-0672 (2017-2021) to the CBGP). In the frame of this latter program R. T. was supported with a postdoctoral contract. We are in debt with J. Berlanga for the use of the gradient fractionation system and with P. Olivares and I. Díaz for her assistance. We deeply thank G. Hernández, A. Ferrando, J. Berlanga and F. García-Arenal for their helpful comments on the manuscript.

## References

1. Jackson RJ, Hellen CU, Pestova TV. The mechanism of eukaryotic translation initiation and principles of its regulation. Nat Rev Mol Cell Biol. 2010; 11:113–127. DOI: 10.1038/nrm2838 [PubMed: 20094052]
2. Sonenberg N, Hinnebusch AG. Regulation of translation initiation in eukaryotes: mechanisms and biological targets. Cell. 2009; 136:731–745. DOI: 10.1016/j.cell.2009.01.042 [PubMed: 19239892]
3. Hinnebusch AG, Ivanov IP, Sonenberg N. Translational control by 5'-untranslated regions of eukaryotic mRNAs. Science. 2016; 352:1413–1416. DOI: 10.1126/science.aad9868 [PubMed: 27313038]
4. Peter D, et al. Molecular architecture of 4E-BP translational inhibitors bound to eIF4E. Molecular cell. 2015; 57:1074–1087. DOI: 10.1016/j.molcel.2015.01.017 [PubMed: 25702871]
5. Hernandez G, Altmann M, Lasko P. Origins and evolution of the mechanisms regulating translation initiation in eukaryotes. Trends Biochem Sci. 2010; 35:63–73. DOI: 10.1016/j.tibs.2009.10.009 [PubMed: 19926289]
6. Poulin F, Gingras AC, Olsen H, Chevalier S, Sonenberg N. 4E-BP3, a new member of the eukaryotic initiation factor 4E-binding protein family. The Journal of biological chemistry. 1998; 273:14002–14007. [PubMed: 9593750]
7. Pause A, et al. Insulin-dependent stimulation of protein synthesis by phosphorylation of a regulator of 5'-cap function. Nature. 1994; 371:762–767. DOI: 10.1038/371762a0 [PubMed: 7935836]
8. Lin TA, et al. PHAS-I as a link between mitogen-activated protein kinase and translation initiation. Science. 1994; 266:653–656. [PubMed: 7939721]
9. Cosentino GP, et al. Eap1p, a novel eukaryotic translation initiation factor 4E-associated protein in Saccharomyces cerevisiae. Mol Cell Biol. 2000; 20:4604–4613. [PubMed: 10848587]
10. Altmann M, Schmitz N, Berset C, Trachsel H. A novel inhibitor of cap-dependent translation initiation in yeast: p20 competes with eIF4G for binding to eIF4E. The EMBO journal. 1997; 16:1114–1121. DOI: 10.1093/emboj/16.5.1114 [PubMed: 9118949]
11. Nelson MR, Leidal AM, Smibert CA. Drosophila Cup is an eIF4E-binding protein that functions in Smaug-mediated translational repression. The EMBO journal. 2004; 23:150–159. DOI: 10.1038/sj.emboj.7600026 [PubMed: 14685270]
12. Jung MY, Lorenz L, Richter JD. Translational control by neuroguidin, a eukaryotic initiation factor 4E and CPEB binding protein. Mol Cell Biol. 2006; 26:4277–4287. DOI: 10.1128/MCB.02470-05 [PubMed: 16705177]
13. Mayberry LK, et al. Plant cap binding complexes eukaryotic initiation factors eIF4F and eIFiso4F: molecular specificity of subunit binding. The Journal of biological chemistry. 2011; doi: 10.1074/jbc.M111.280099

14. Browning KS, Bailey-Serres J. Mechanism of cytoplasmic mRNA translation. Arabidopsis Book. 2015; 13:e0176.doi: 10.1199/tab.0176 [PubMed: 26019692]
15. Bush MS, et al. Selective recruitment of proteins to 5' cap complexes during the growth cycle in Arabidopsis. The Plant journal : for cell and molecular biology. 2009; 59:400–412. DOI: 10.1111/j.1365-313X.2009.03882.x [PubMed: 19453450]
16. Yanguez E, Castro-Sanz AB, Fernandez-Bautista N, Oliveros JC, Castellano MM. Analysis of genome-wide changes in the translatome of Arabidopsis seedlings subjected to heat stress. PloS one. 2013; 8:e71425.doi: 10.1371/journal.pone.0071425 [PubMed: 23977042]
17. Echevarria-Zomeno S, et al. Regulation of Translation Initiation under Biotic and Abiotic Stresses. International journal of molecular sciences. 2013; 14:4670–4683. DOI: 10.3390/ijms14034670 [PubMed: 23443165]
18. Merchante C, Stepanova AN, Alonso JM. Translation regulation in plants: an interesting past, an exciting present and a promising future. The Plant journal : for cell and molecular biology. 2017; 90:628–653. DOI: 10.1111/tpj.13520 [PubMed: 28244193]
19. Missra A, et al. The Circadian Clock Modulates Global Daily Cycles of mRNA Ribosome Loading. The Plant cell. 2015; 27:2582–2599. DOI: 10.1105/tpc.15.00546 [PubMed: 26392078]
20. Piques M, et al. Ribosome and transcript copy numbers, polysome occupancy and enzyme dynamics in Arabidopsis. Molecular systems biology. 2009; 5:314.doi: 10.1038/msb.2009.68 [PubMed: 19888209]
21. Pal SK, et al. Diurnal changes of polysome loading track sucrose content in the rosette of wild-type arabidopsis and the starchless pgm mutant. Plant physiology. 2013; 162:1246–1265. DOI: 10.1104/pp.112.212258 [PubMed: 23674104]
22. Sesma A, Castresana C, Castellano MM. Regulation of Translation by TOR, eIF4E and eIF2alpha in Plants: Current Knowledge, Challenges and Future Perspectives. Frontiers in plant science. 2017; 8:644.doi: 10.3389/fpls.2017.00644 [PubMed: 28491073]
23. Munoz A, Castellano MM. Regulation of Translation Initiation under Abiotic Stress Conditions in Plants: Is It a Conserved or Not so Conserved Process among Eukaryotes? Comp Funct Genomics. 2012; 2012doi: 10.1155/2012/406357
24. Toribio, R, , et al. Evolution of the Protein Synthesis Machinery and Its Regulation. Hernández, G, Jagus, R, editors. Springer; 2016.
25. Hernandez G, et al. Mextli is a novel eukaryotic translation initiation factor 4E-binding protein that promotes translation in Drosophila melanogaster. Mol Cell Biol. 2013; 33:2854–2864. DOI: 10.1128/MCB.01354-12 [PubMed: 23716590]
26. Freire MA, et al. Plant lipoxygenase 2 is a translation initiation factor-4E-binding protein. Plant Mol Biol. 2000; 44:129–140. [PubMed: 11117257]
27. Freire MA. Translation initiation factor (iso) 4E interacts with BTF3, the beta subunit of the nascent polypeptide-associated complex. Gene. 2005; 345:271–277. DOI: 10.1016/j.gene.2004.11.030 [PubMed: 15716105]
28. Lázaro-Mixteco PE, Dinkova TD. Identification of Proteins from Cap-Binding Complexes by Mass Spectrometry During Maize (Zea mays L.) Germination. J Mex Chem Soc. 2012; 56:36–54.
29. Patrick RM, et al. Discovery and characterization of conserved binding of eIF4E 1 (CBE1), a eukaryotic translation initiation factor 4E-binding plant protein. The Journal of biological chemistry. 2018; 293:17240–17247. DOI: 10.1074/jbc.RA118.003945 [PubMed: 30213859]
30. Wu Z, et al. Regulation of plant immune receptor accumulation through translational repression by a glycine-tyrosine-phenylalanine (GYF) domain protein. eLife. 2017; 6doi: 10.7554/eLife.23684
31. Tarun SZ Jr, Sachs AB. A common function for mRNA 5' and 3' ends in translation initiation in yeast. Genes & development. 1995; 9:2997–3007. [PubMed: 7498795]
32. Wells SE, Hillner PE, Vale RD, Sachs AB. Circularization of mRNA by eukaryotic translation initiation factors. Molecular cell. 1998; 2:135–140. [PubMed: 9702200]
33. Gallie DR. Plant growth and fertility requires functional interactions between specific PABP and eIF4G gene family members. PloS one. 2018; 13:e0191474.doi: 10.1371/journal.pone.0191474 [PubMed: 29381712]

34. O'Malley RC, Ecker JR. Linking genotype to phenotype using the Arabidopsis unimutant collection. The Plant journal : for cell and molecular biology. 2010; 61:928–940. DOI: 10.1111/j.1365-313X.2010.04119.x [PubMed: 20409268]
35. Krysan PJ, Young JC, Sussman MR. T-DNA as an insertional mutagen in Arabidopsis. The Plant cell. 1999; 11:2283–2290. DOI: 10.1105/tpc.11.12.2283 [PubMed: 10590158]
36. Merchante C, et al. Gene-specific translation regulation mediated by the hormone-signaling molecule EIN2. Cell. 2015; 163:684–697. DOI: 10.1016/j.cell.2015.09.036 [PubMed: 26496608]
37. Hsu PY, et al. Super-resolution ribosome profiling reveals unannotated translation events in Arabidopsis. Proceedings of the National Academy of Sciences of the United States of America. 2016; doi: 10.1073/pnas.1614788113
38. Juntawong P, Girke T, Bazin J, Bailey-Serres J. Translational dynamics revealed by genome-wide profiling of ribosome footprints in Arabidopsis. Proceedings of the National Academy of Sciences of the United States of America. 2014; 111:E203–212. DOI: 10.1073/pnas.1317811111 [PubMed: 24367078]
39. Wang WH, et al. Regulation of the calcium-sensing receptor in both stomatal movement and photosynthetic electron transport is crucial for water use efficiency and drought tolerance in Arabidopsis. Journal of experimental botany. 2014; 65:223–234. DOI: 10.1093/jxb/ert362 [PubMed: 24187420]
40. South PF, et al. Bile Acid Sodium Symporter BASS6 Can Transport Glycolate and Is Involved in Photorespiratory Metabolism in Arabidopsis thaliana. The Plant cell. 2017; 29:808–823. DOI: 10.1105/tpc.16.00775 [PubMed: 28351992]
41. El-Zohri M, Odjegba V, Ma L, Rathinasabapathi B. Sulfate influx transporters in Arabidopsis thaliana are not involved in arsenate uptake but critical for tissue nutrient status and arsenate tolerance. Planta. 2015; 241:1109–1118. DOI: 10.1007/s00425-015-2241-4 [PubMed: 25600998]
42. Dar AA, Choudhury AR, Kancharla PK, Arumugam N. The FAD2 Gene in Plants: Occurrence, Regulation, and Role. Frontiers in plant science. 2017; 8:1789.doi: 10.3389/fpls.2017.01789 [PubMed: 29093726]
43. Sperling P, Zahringer U, Heinz E. A sphingolipid desaturase from higher plants. Identification of a new cytochrome b5 fusion protein. The Journal of biological chemistry. 1998; 273:28590–28596. DOI: 10.1074/jbc.273.44.28590 [PubMed: 9786850]
44. Aluri S, Buttner M. Identification and functional expression of the Arabidopsis thaliana vacuolar glucose transporter 1 and its role in seed germination and flowering. Proceedings of the National Academy of Sciences of the United States of America. 2007; 104:2537–2542. DOI: 10.1073/pnas.0610278104 [PubMed: 17284600]
45. Lellis AD, et al. eIFiso4G augments the synthesis of specific plant proteins involved in normal chloroplast function. Plant physiology. 2019; doi: 10.1104/pp.19.00557
46. Lellis AD, et al. Deletion of the eIFiso4G subunit of the Arabidopsis eIFiso4F translation initiation complex impairs health and viability. Plant Mol Biol. 2010; 74:249–263. DOI: 10.1007/s11103-010-9670-z [PubMed: 20694742]
47. Bi C, et al. Arabidopsis translation initiation factors eIFiso4G1/2 link repression of mRNA cap-binding complex eIFiso4F assembly with RNA-binding protein SOAR1-mediated ABA signaling. The New phytologist. 2019; 223:1388–1406. DOI: 10.1111/nph.15880 [PubMed: 31050354]
48. Cho HY, Lu MJ, Shih MC. The SnRK1-eIFiso4G1 signaling relay regulates the translation of specific mRNAs in Arabidopsis under submergence. The New phytologist. 2019; 222:366–381. DOI: 10.1111/nph.15589 [PubMed: 30414328]
49. Tajima Y, et al. Requirement for eukaryotic translation initiation factors in cap-independent translation differs between bipartite genomic RNAs of red clover necrotic mosaic virus. Virology. 2017; 509:152–158. DOI: 10.1016/j.virol.2017.06.015 [PubMed: 28646650]
50. Lellis AD, Kasschau KD, Whitham SA, Carrington JC. Loss-of-susceptibility mutants of Arabidopsis thaliana reveal an essential role for eIF(iso)4E during potyvirus infection. Current biology : CB. 2002; 12:1046–1051. [PubMed: 12123581]
51. Duprat A, et al. The Arabidopsis eukaryotic initiation factor (iso)4E is dispensable for plant growth but required for susceptibility to potyviruses. The Plant journal : for cell and molecular biology. 2002; 32:927–934. [PubMed: 12492835]

Europe PMC Funders Author Manuscripts


52. Callot C, Gallois JL. Pyramiding resistances based on translation initiation factors in Arabidopsis is impaired by male gametophyte lethality. Plant signaling & behavior. 2014; 9:e27940.doi: 10.4161/psb.27940 [PubMed: 24492391]
53. Fritz-Laylin LK, Krishnamurthy N, Tor M, Sjolander KV, Jones JD. Phylogenomic analysis of the receptor-like proteins of rice and Arabidopsis. Plant physiology. 2005; 138:611–623. DOI: 10.1104/pp.104.054452 [PubMed: 15955925]
54. Stebbins-Boaz B, Cao Q, de Moor CH, Mendez R, Richter JD. Maskin is a CPEB-associated factor that transiently interacts with elF-4E. Molecular cell. 1999; 4:1017–1027. [PubMed: 10635326]
55. Duncan R, Milburn SC, Hershey JW. Regulated phosphorylation and low abundance of HeLa cell initiation factor eIF-4F suggest a role in translational control. Heat shock effects on eIF-4F. The Journal of biological chemistry. 1987; 262:380–388. [PubMed: 3793730]
56. Gonzalez A, Hall MN. Nutrient sensing and TOR signaling in yeast and mammals. The EMBO journal. 2017; 36:397–408. DOI: 10.15252/embj.201696010 [PubMed: 28096180]
57. Deprost D, et al. The Arabidopsis TOR kinase links plant growth, yield, stress resistance and mRNA translation. EMBO Rep. 2007; 8:864–870. DOI: 10.1038/sj.embor.7401043 [PubMed: 17721444]
58. Sormani R, et al. Saccharomyces cerevisiae FKBP12 binds Arabidopsis thaliana TOR and its expression in plants leads to rapamycin susceptibility. BMC plant biology. 2007; 7:26.doi: 10.1186/1471-2229-7-26 [PubMed: 17543119]
59. Dobrenel T, et al. The Arabidopsis TOR Kinase Specifically Regulates the Expression of Nuclear Genes Coding for Plastidic Ribosomal Proteins and the Phosphorylation of the Cytosolic Ribosomal Protein S6. Frontiers in plant science. 2016; 7:1611.doi: 10.3389/fpls.2016.01611 [PubMed: 27877176]
60. Lee DH, Park SJ, Ahn CS, Pai HS. MRF Family Genes Are Involved in Translation Control, Especially under Energy-Deficient Conditions, and Their Expression and Functions Are Modulated by the TOR Signaling Pathway. The Plant cell. 2017; 29:2895–2920. DOI: 10.1105/tpc.17.00563 [PubMed: 29084871]
61. Alonso JM, et al. Genome-wide insertional mutagenesis of Arabidopsis thaliana. Science. 2003; 301:653–657. DOI: 10.1126/science.1086391 [PubMed: 12893945]
62. Curtis MD, Grossniklaus U. A gateway cloning vector set for high-throughput functional analysis of genes in planta. Plant physiology. 2003; 133:462–469. DOI: 10.1104/pp.103.027979 [PubMed: 14555774]
63. Nakagawa T, et al. Development of series of gateway binary vectors, pGWBs, for realizing efficient construction of fusion genes for plant transformation. Journal of Bioscience and Bioengineering. 2007; 104:34–41. DOI: 10.1263/jbb.104.34 [PubMed: 17697981]
64. Nakamura S, et al. Gateway binary vectors with the bialaphos resistance gene, bar, as a selection marker for plant transformation. Bioscience, biotechnology, and biochemistry. 2010; 74:1315–1319. DOI: 10.1271/bbb.100184
65. Nakagawa T, et al. Improved Gateway binary vectors: high-performance vectors for creation of fusion constructs in transgenic analysis of plants. Bioscience, biotechnology, and biochemistry. 2007; 71:2095–2100. DOI: 10.1271/bbb.70216
66. Rossignol P, Collier S, Bush M, Shaw P, Doonan JH. Arabidopsis POT1A interacts with TERT-V(I8), an N-terminal splicing variant of telomerase. J Cell Sci. 2007; 120:3678–3687. DOI: 10.1242/jcs.004119 [PubMed: 17911168]
67. Munoz A, et al. RIMA-Dependent Nuclear Accumulation of IYO Triggers Auxin-Irreversible Cell Differentiation in Arabidopsis. The Plant cell. 2017; 29:575–588. DOI: 10.1105/tpc.16.00791 [PubMed: 28223441]
68. Echevarria-Zomeno S, et al. Dissecting the proteome dynamics of the early heat stress response leading to plant survival or death in Arabidopsis. Plant Cell and Environment. 2015; 39:1264–1278. DOI: 10.1111/pce.12664
69. Fernandez-Bautista N, Fernandez-Calvino L, Munoz A, Castellano MM. HOP3, a member of the HOP family in Arabidopsis, interacts with BiP and plays a major role in the ER stress response. Plant, cell & environment. 2017; 40:1341–1355. DOI: 10.1111/pce.12927

70. Munoz A, Castellano MM. Coimmunoprecipitation of Interacting Proteins in Plants. Methods in molecular biology. 2018; 1794:279–287. DOI: 10.1007/978-1-4939-7871-7_19 [PubMed: 29855965]
71. Castellano MM, Sablowski R. Phosducin-Like Protein 3 is required for microtubule-dependent steps of cell division but not for meristem growth in Arabidopsis. The Plant cell. 2008; 20:969–981. DOI: 10.1105/tpc.107.057737 [PubMed: 18390592]
72. Fernandez-Bautista N, et al. HOP family plays a major role in long-term acquired thermotolerance in Arabidopsis. Plant, cell & environment. 2018; 41:1852–1869. DOI: 10.1111/pce.13326
73. Friedman DB. Quantitative proteomics for two-dimensional gels using difference gel electrophoresis. Methods in molecular biology. 2007; 367:10.
74. Pearson WR, Wood T, Zhang Z, Miller W. Comparison of DNA sequences with protein sequences. Genomics. 1997; 46:24–36. DOI: 10.1006/geno.1997.4995 [PubMed: 9403055]
75. Kim D, et al. TopHat2: accurate alignment of transcriptomes in the presence of insertions, deletions and gene fusions. Genome biology. 2013; 14:R36.doi: 10.1186/gb-2013-14-4-r36 [PubMed: 23618408]
76. Wickham, H. ggplot2: Elegant Graphics for Data Analysis. Springer-Verlag; New York: 2016.
77. Popa A, et al. RiboProfiling: a Bioconductor package for standard Ribo-seq pipeline processing. F1000Research. 2016; 5
78. Lawrence M, et al. Software for computing and annotating genomic ranges. PLoS computational biology. 2013; 9(8):e1003118. [PubMed: 23950696]
79. Hardcastle, TJ. riboSeqR: Analysis of sequencing data from ribosome profiling experiments. 2014. R package version 1.2.0. <https://bioconductor.riken.jp/packages/3.1/bioc/html/riboSeqR.html>
80. Morgan, M; Pagès, H; Obenchain, V; Hayden, N. Rsamtools: Binary alignment (BAM), FASTA, variant call (BCF), and tabix file import. 2018. R package version 1.32.0, <http://bioconductor.org/packages/release/bioc/html/Rsamtools.html>
81. Love MI, Huber W, Anders S. Moderated estimation of fold change and dispersion for RNA-seq data with DESeq2. Genome biology. 2014; 15:1.


Europe PMC Funders Author Manuscripts

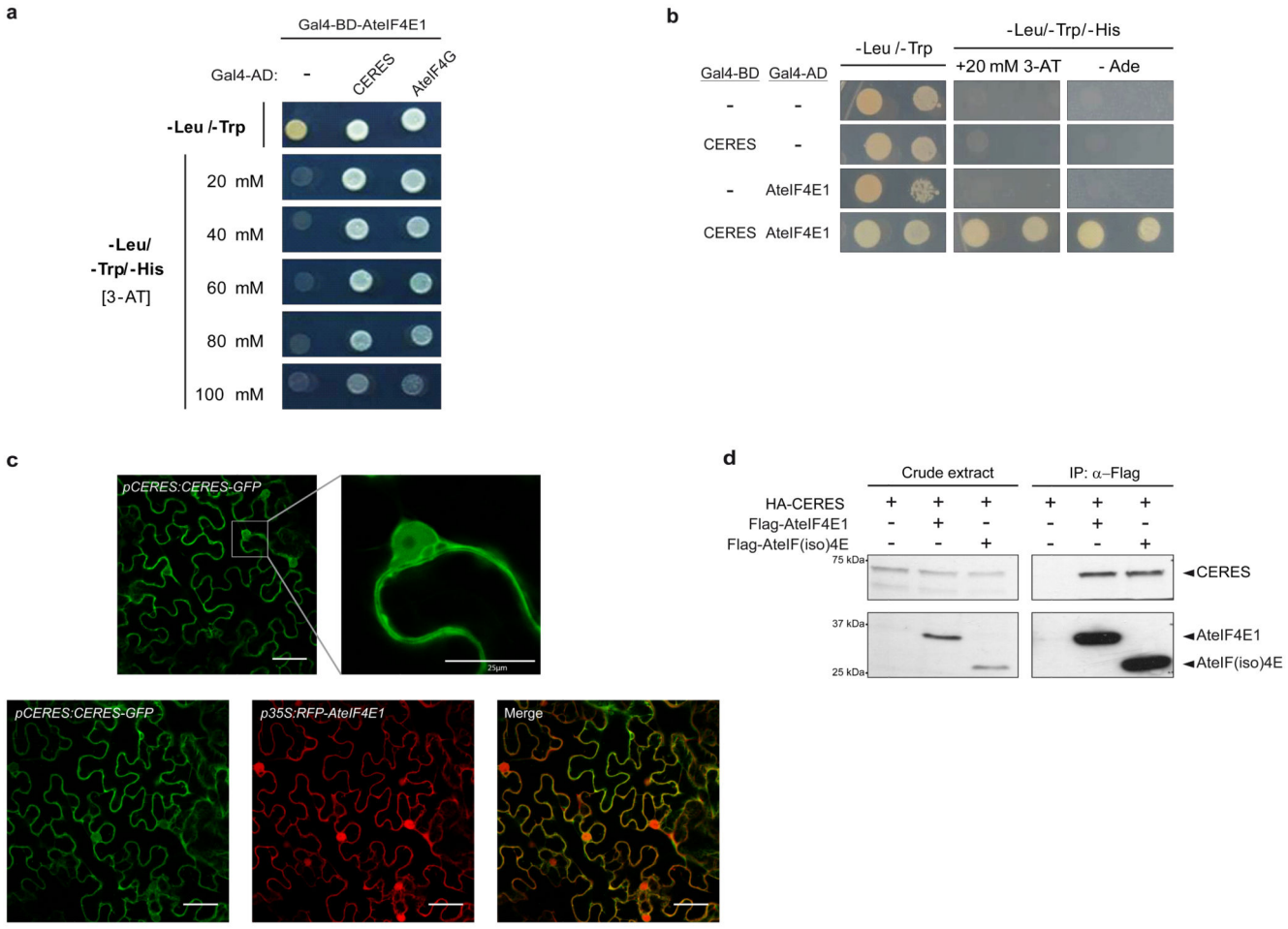


**Figure 1. CERES interacts with AteIF4E1.**

(**a**) Growth in different selection media of the original clones isolated from the yeast two-hybrid screening used to identify potential interactors of AteIF4E1. These clones harboured AteIF4E1 (fused to the Gal4 DNA binding domain, Gal4-BD) and partial clones of either CERES or eIF4G (fused to the Gal4 activation domain, Gal4-AD). As control the same yeast strain used for the screening (which expressed AteIF4E1-Gal4-BD) was co-transformed with a construct that expressed a bare Gal4-AD. (**b**) Directed yeast two-hybrid assay to analyse CERES (full length) interaction with AteIF4E1. (**c**) Subcellular localisation analysis of CERES-GFP (upper panel) and co-localisation analysis of CERES-GFP and RFP-AteIF4E1 (lower panel) in *N. benthamiana* leaves. Scale bars correspond to 50 µm, except the bar in the upper right panel that corresponds to 25 µm. (**d**) Co-immunoprecipitation analysis from *N. benthamiana* leaves transiently expressing under the control of the *35S* promoter different combinations of HA-CERES, Flag-AteIF4E1 and Flag-AteIF(iso)4E. The presence of the different proteins in the crude extracts and in the eluted fractions from the immunoprecipitations (IP: α-Flag) was analysed by western-blot using the anti-HA and anti-Flag antibodies. The experiments in (**b**) and (**a, c-d**) were independently repeated four and three times, respectively with similar results.




Europe PMC Funders Author Manuscripts

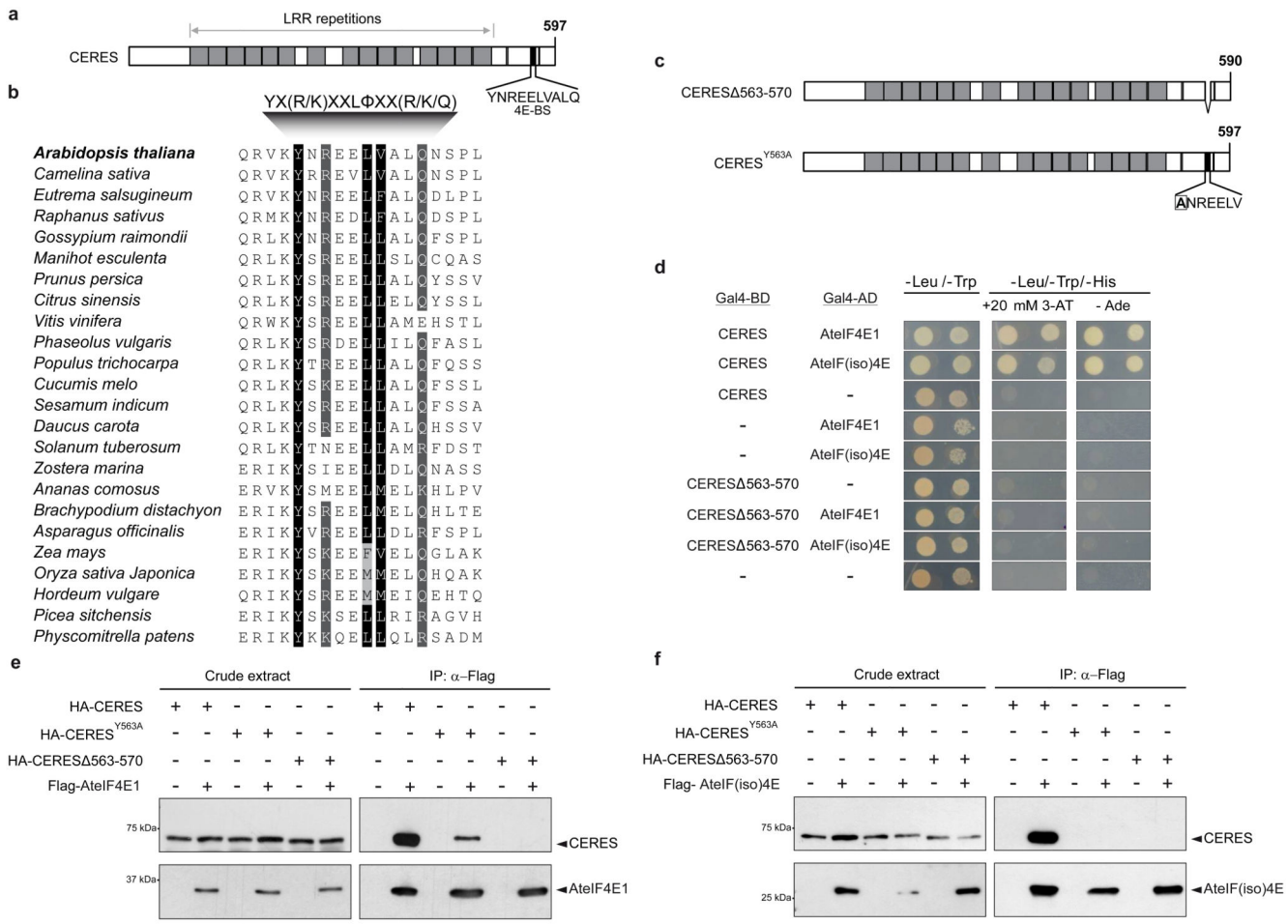


**Figure 2. The 4E-BS is highly conserved in plants and is essential for CERES interaction with AteIF4E isoforms.**

(**a**) Schematic representation of CERES´ structure. (**b**) Sequence conservation of the extended 4E-BS in different CERES orthologues in the plant kingdom. The consensus extended sequence for 4E-BS is shown in the upper part of the panel. (**c**) Schematic representations of CERES deletion CERESΔ563-570 and CERES point mutation Y653A (CERES$^{Y653A}$) used for further analysis. (**d**) Yeast two-hybrid analysis to evaluate the relevance of the 4E-BS in the interaction with the eIF4E isoforms. The proteins fused to the Gal4-BD and Gal4-AD that were co-expressed in the AH109 strain are shown on the left of the panel. Independent transformants were tested for growth in non-selective medium (-Leu-Trp) or prototrophy-selective medium (-Leu, -Trp, -His) in the presence of 3-AT or in the absence of adenine (-Ade). The constructs expressing the bare Gal4-BD and Gal4-AD were used as controls (-). (**e-f**) Co-immunoprecipitation analysis from *N. benthamiana* leaves transiently expressing, under the control of the *35S* promoter, different combinations of the HA-CERES (full-length/wild type and the versions described in (**c**)) and Flag-AteIF4E1 (**e**) or Flag-AteIF(iso)4E (**f**). The presence of the different proteins in the crude extracts and in the eluted fractions (IP: α-Flag) was analysed by western-blot using the anti-HA and anti-Flag antibodies. The experiments in (**d-f**) were repeated independently three times with similar results.

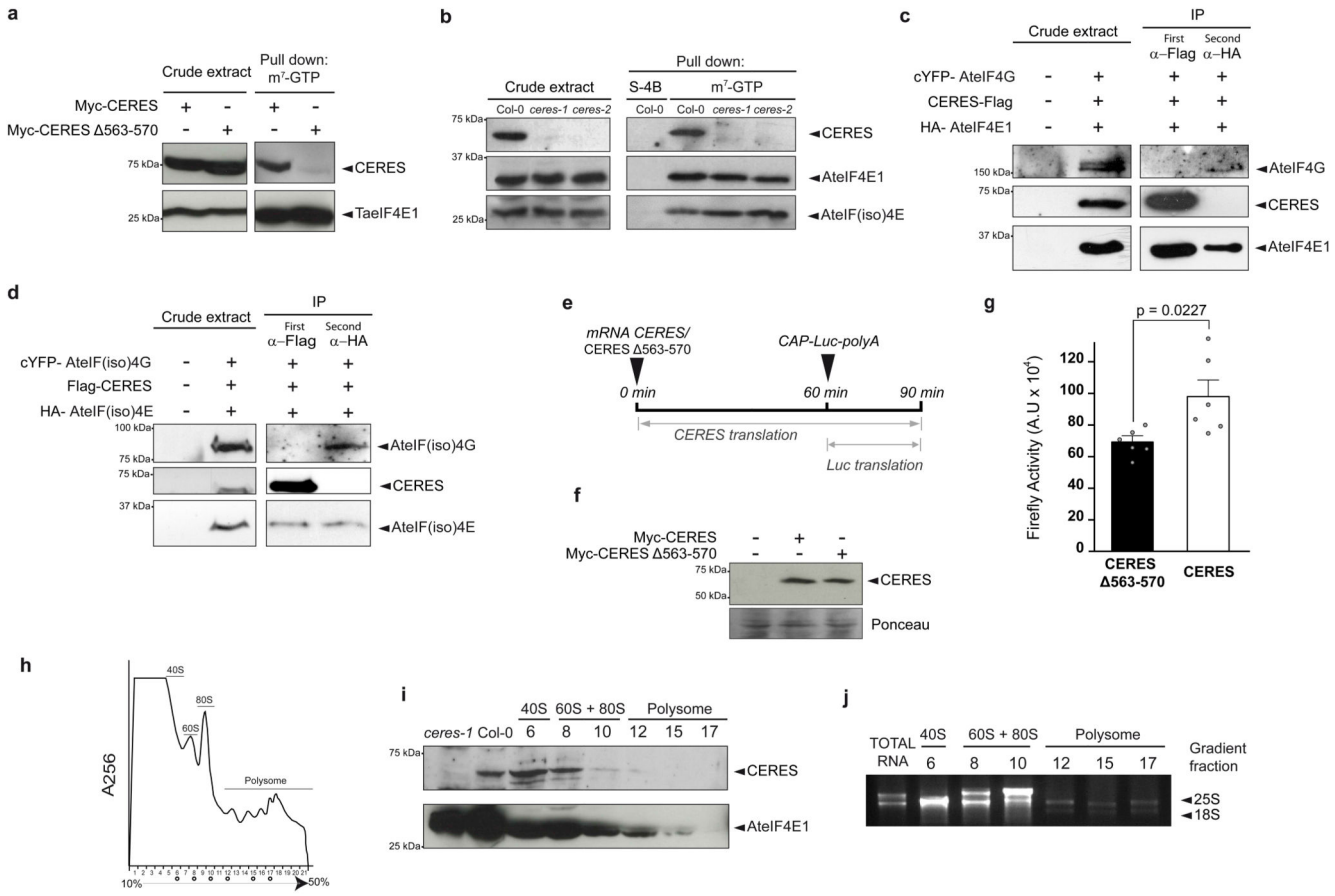


**Figure 3. CERES, through its interaction with eIF4E, forms complexes that bind the cap structure in the absence of eIF4G isoforms, promotes translation of a reporter mRNA and co-sediments along with eIF4E1 in translation initiation complexes.**

(**a**) Pull-down using 7-methyl-GTP-Sepharose from WGE extracts expressing either CERES full-length or CERESΔ563-570 fused to Myc. The presence of the different proteins in the crude extracts and in the eluted fractions (Pull down: $m^7$-GTP) was analysed by western-blot using the anti-Myc and anti-TaeIF4E antibodies. (**b**) Pull down of extracts from seedlings of Col-0, *ceres-1* and *ceres-2* mutants using either Sepharose-4B (S-4B) or 7-methyl-GTP-Sepharose 4B ($m^7$-GTP). The presence of CERES, eIF4E1 or eIF(iso4E) in the crude extracts and in the different pull downs were analysed by western-blot using specific antibodies against AtCERES, AteIF4E1 and AteIF(iso)4E. (**c-d**) Sequential co-immunoprecipitation assays from *N. benthamiana* leaves transiently expressing, under the control of the *35S* promoter, cYFP-eIF4G, CERES-Flag and HA-AteIF4E1 (**c**), or cYFP-eIF(iso)4G, Flag-CERES and HA-eIF(iso)4E (**d**). The corresponding extracts were subjected to a first co-immunoprecipitation using anti-Flag beads and the flow-through of this co-immunoprecipitation was further subjected to a second co-immunoprecipitation using anti-HA beads. The presence of the different proteins in the crude extracts and in the eluted fractions was analysed by western-blot using the anti-GFP, anti-Flag and anti-HA antibodies. (**e-g**) *In vitro* translation assay of a reporter mRNA in the presence of either full-length CERES or a version of CERES that lacks the 4E-BS (CERESΔ563-570). (**e**) Schematic




Europe PMC Funders Author Manuscripts

representation of the *in vitro* translation assay performed in this analysis. The full-length *CERES* or *CERESΔ563-570* mRNAs were translated in WGE for 60 min. At that point, a capped reporter *Fluc* mRNA was added to both extracts. Translation was stopped 30 min after the addition of the reporter mRNA. (**f**) Accumulation of CERES versions in the assay was analysed by western-blot using the anti-Myc antibody. (**g**) Fluc activity in both extracts was measured and represented as means ± SEM (n = 6 independent experiments). The asterisk highlights statistical difference ($p<0.0227$) using unpaired two sided t test and Kolmogorov–Smirnov test for normal distribution analysis. (**h-j**) Analysis of the distribution of CERES in different fractions of a polysome sucrose gradient. (**h**) Polysome profile of wild-type plants. Ribonucleoprotein material (RNP) was extracted from Col-0 seedlings and resolved on a 10-50% sucrose gradient. Absorbance at 256 nm was continuously monitored through the different fractions of the gradient. Fractions 6, 8, 10, 12, 15 and 17 were selected for further analyses. (**i**) Western-blot of protein extracts derived from equal volumes of the selected fractions using anti-AtCERES and anti-AteIF4E1 antibodies. Total protein extracts from *ceres-1* mutant and Col-0 were included as controls. (**j**) In order to corroborate the ribosomal nature of the selected fractions, total RNA (before sucrose gradient fractionation) and RNA obtained from equal volumes of the selected fractions was subjected to electrophoretic analysis. According to the polysomal profile and the distribution of 18S and 25S rRNAs, fraction 6 corresponded to 40S complexes, fractions 8 and 10 were enriched in 60S+80S complexes, while fractions 12, 15 and 17 corresponded to polysomes. The experiments in (**a-d, f, h-j**) were repeated independently three times with similar results.



Europe PMC Funders Author Manuscripts

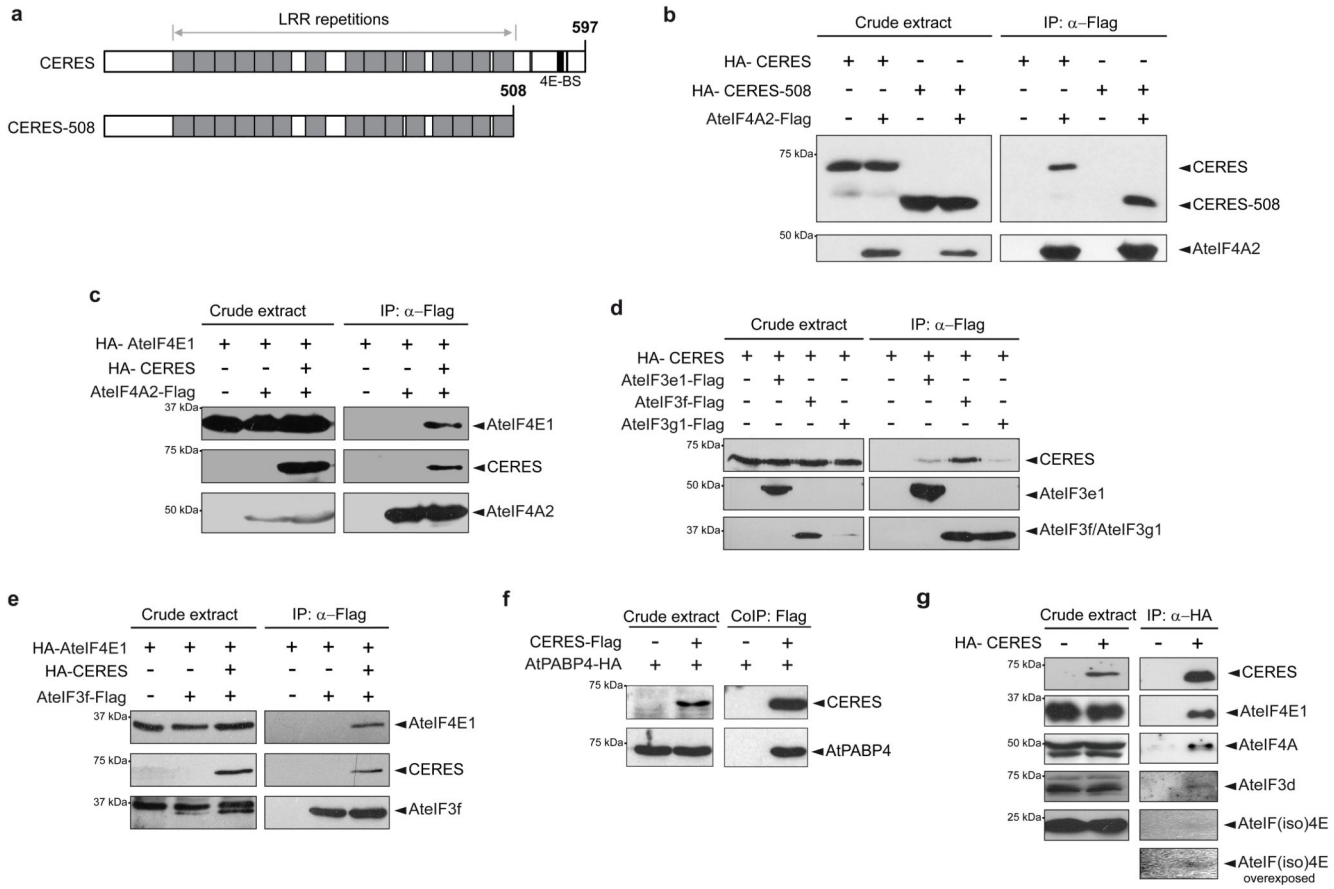


**Figure 4. CERES interacts *in vivo* with eIF4A, eIF3 and PABP.**

(**a**) Schematic representation of CERES and the truncated version CERES-508 used in this study. (**b-f**) Co-immunoprecipitation analysis from *N. benthamiana* leaves transiently expressing, under the control of the *35S* promoter, different combinations of HA-CERES, HA-CERES-508 and AteIF4A2-Flag (**b**); HA-AteIF4E1, HA-CERES and AteIF4A2-Flag (**c**); HA-CERES, AteIF3e1-Flag, AteIF3f-Flag and AteIF3g1-Flag (**d**); HA-AteIF4E1, HA-CERES and AteIF3f-Flag (**e**) and CERES-Flag and AtPABP4-HA (**f**). The presence of the different proteins in the crude extracts and in the eluted fractions from the immunoprecipitations (IP: α-Flag) was analysed by western-blot using the anti-HA and anti-Flag antibodies. (**g**) Immunoprecipitation assay (IP: α-HA) from extracts of Col-0 (-) and from Arabidopsis seedlings expressing HA-CERES under the control of the constitutive promoter *35S* and of the translational enhancer *Ω sequence.* The presence of the different proteins in the crude extracts and in the eluted fractions from the immunoprecipitation was analysed by western-blot using the anti-AtCERES, anti-AteIF4A, anti-AteIF4E1, anti-human eIF3D and anti-AteIF(iso)4E antibodies. An overexposure of the western blot with anti-AteIF(iso)4E is shown at the bottom of the figure. The experiments in (**b-g**) were repeated independently three times with similar results.




Europe PMC Funders Author Manuscripts

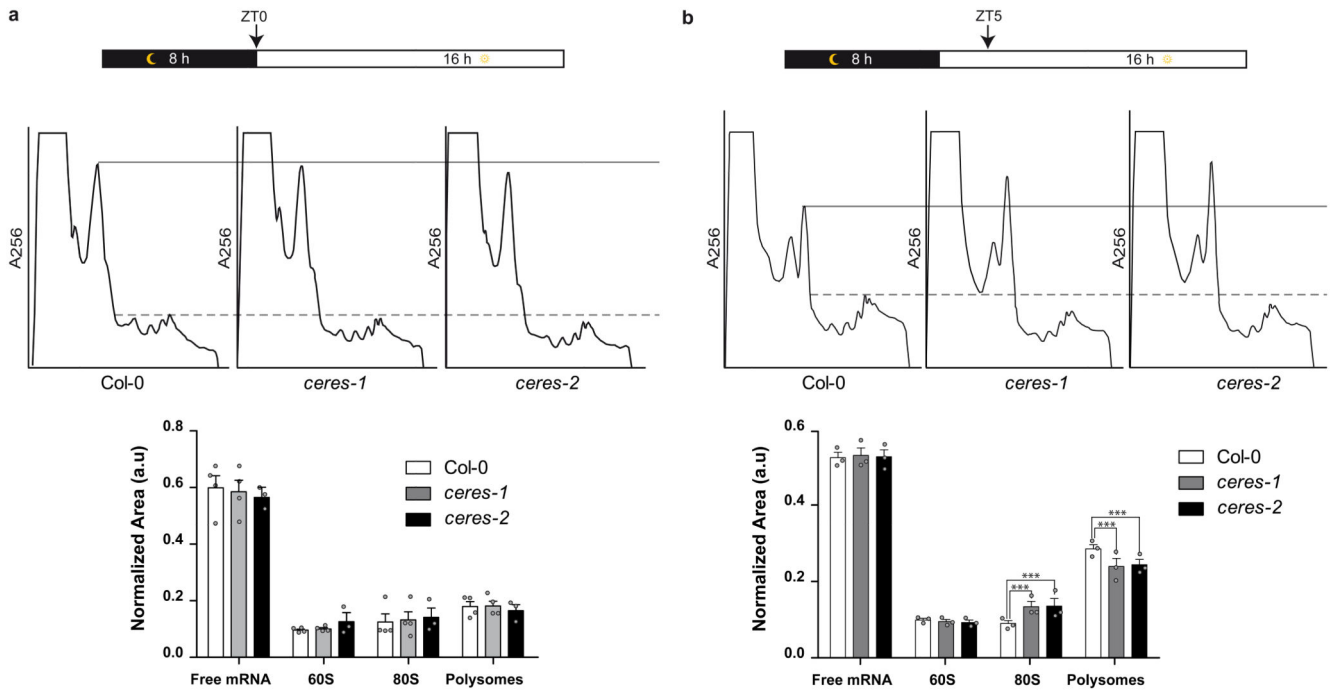


**Figure 5. CERES modulates translation at specific stages of the diel cycle.**

Schematic representation of the two different time-points ZT0 and ZT5 (**a** and **b**, upper panel, respectively) that have been analysed during the 16 h-light/ 8 h-dark cycle. Representative polysome profiles of Col-0, *ceres-1* and *ceres-2* seedlings at ZT0 and ZT5 (**a** and **b**, middle panel, respectively). Quantification of the polysome profile areas that correspond to free mRNA (light density fractions not resolved in the profile), 60S, 80S and polysomes at ZT0 and at ZT5 (**a** and **b**, lower panel, respectively). Values are shown as means ± SEM from n=4 independent experiments for Col-0 and *ceres-1* mutant and n=3 for *ceres-2* mutant in (**a**) and n=3 independent experiments for Col-0, *ceres-1* and *ceres-2* mutants in (**b**). Statistical differences ($p<0.001$) using the two-way ANOVA test are highlighted by asterisks.




Europe PMC Funders Author Manuscripts

Europe PMC Funders Author Manuscripts

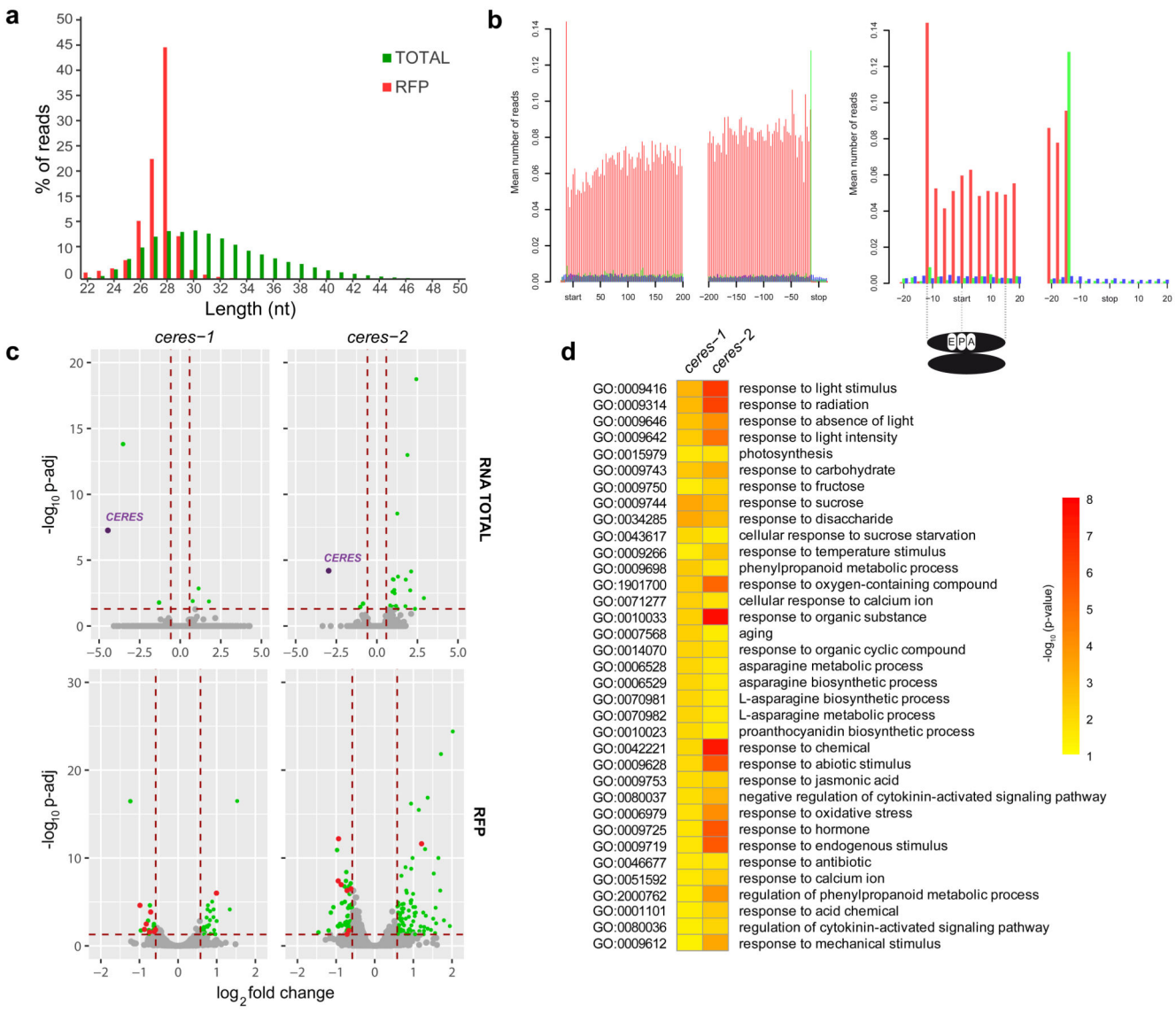


**Figure 6. Super-resolution ribosome profiling analysis of *ceres* mutants.**

(**a**) Size distribution and relative abundance of total RNA and RFP reads. All total RNA and RFP reads from the three assayed genotypes (Col-0, *ceres-1* and *ceres-2*) with their corresponding replicates (n=3 independent experiments) were combined for this analysis. (**b**) Coverage values of 28 nt RFP reads within and close to the Arabidopsis annotated genes (left panel) and the inferred footprint positions related to the initiating ribosomes (right panel). The main frame according to the annotated start codon is shown in red and the two other reading frames are shown in blue and green. (**c**) Volcano plots of total RNA- and RFP-changes (upper and lower panel, respectively) in *ceres-1* and *ceres-2* mutants compared to Col-0 (n=3 independent experiments). Green dots represent significantly upregulated and downregulated genes (absolute total RNA or RFP fold change values of $\log_2 \geq |0.58|$; padj $\leq 0.05$ in each mutant compared to Col-0). Red dots represent the genes significantly upregulated and downregulated in both mutants specifically at the translational level. The

dot corresponding to *CERES* is shown in purple. Grey dots are genes with a non-significant change. For these analyses, the hypothesis testing was performed by a Wald test. Besides the genotype, batch was also considered as a covariate in the model. p-value was adjusted for multiple testing using Benjamini-Hochberg method. (**d**) GO analysis of the genes with significant altered RFP in *ceres-1* and *ceres-2* mutants compared to Col-0 (n=3 independent experiments). This analysis was done using Fisher statistical test for the analysis of p-value. In this case, the p-values were unadjusted for multiple test comparisons. Only common and significant categories (p-value ≤ 0.05) are shown in this figure. Colour code is shown at the right of the panel.



Europe PMC Funders Author Manuscripts

Europe PMC Funders Author Manuscripts

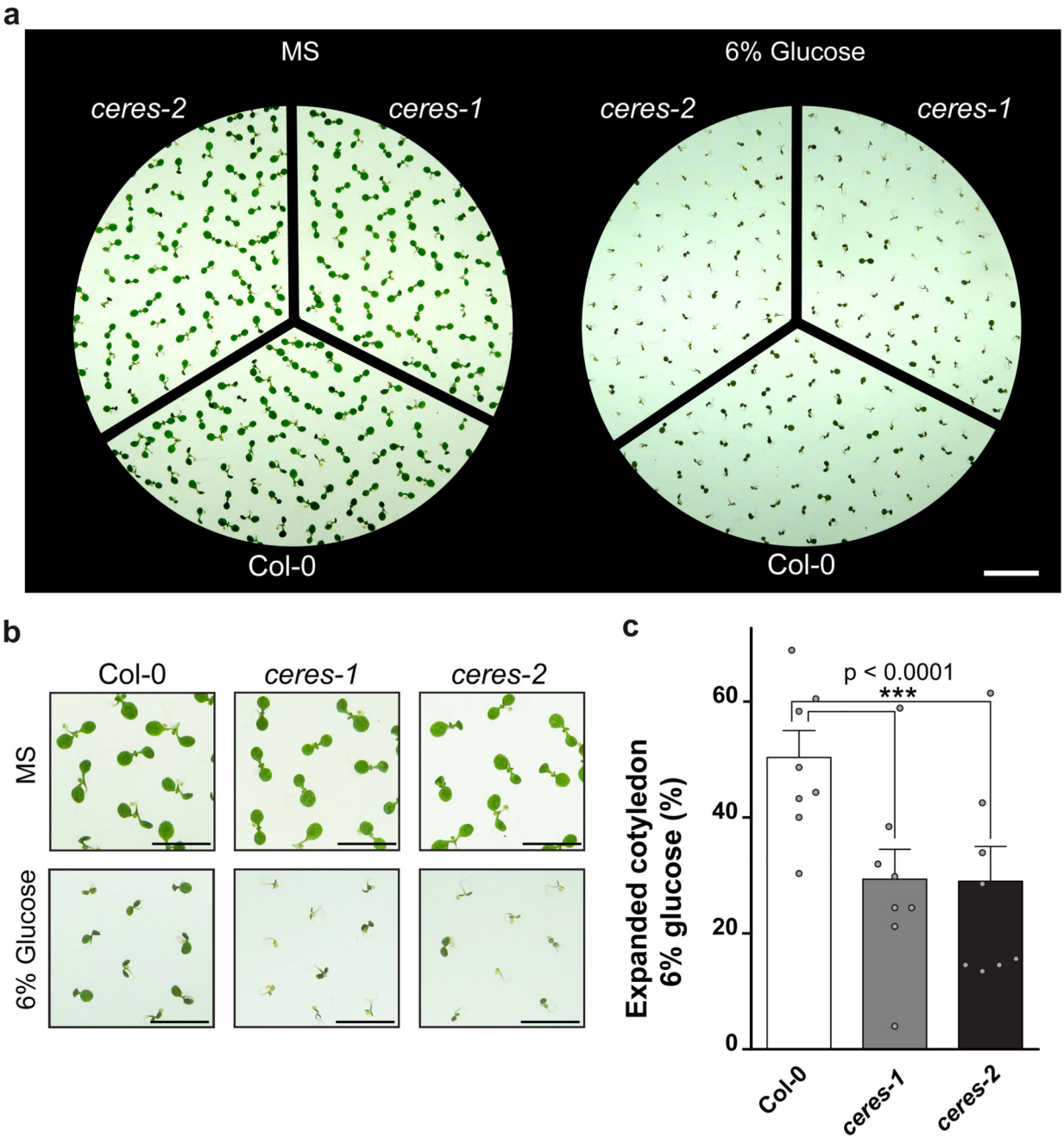


**Figure 7. *ceres* mutants show a hypersensitive phenotype in response to glucose.**

(**a**) Representative growth of Col-0, *ceres-1* and *ceres-2* seedlings in medium lacking glucose (control) or supplemented with 6% glucose for 7 days. (**b**) Close-up views of the upper panel. (**c**) Percentage of seedlings from Col-0, *ceres-1* and *ceres-2* that developed green and expanded cotyledon in the presence of 6% glucose. n=8 independent experiments from three different seed batches were analysed. Values are shown as means ± SEM. Statistical difference between Col-0 and *ceres* mutants ($p < 0.001$) using one-way ANOVA

analysis is highlighted by asterisks. The scale bars in (**a**) and (**b**) correspond to 1.5 cm and 7.5 mm, respectively.



Europe PMC Funders Author Manuscripts